Pathological study of human melioidosis and detection of *Burkholderia pseudomallei* by *in situ* hybridization.

RESEARCH REPORT IN PARTIAL FULFILLMENT OF THE DEGREE OF MASTER OF PATHOLOGY (ANATOMICAL PATHOLOGY)
UNIVERSITY MALAYA
2017

Candidate: Dr Teoh Pak Inn (MGA130005)

Supervisor: Prof Wong Kum Thong

Department of Pathology
Faculty of Medicine
University Malaya

DISCLAIMER AND ACKNOWLEDGEMENT

I hereby declare that the research report is wholly prepared by me, based on research work led by my supervisor, Prof Wong Kum Thong.

I would like to express my greatest gratitude to my supervisor Prof. Wong Kum Thong, for his extraordinary support throughout this difficult project. Without his guidance, expert advice and valuable opinions, the completion of this project may not be possible.

I would also like to thank Dr Hakimah Mahsin (Head of Department, Department of Pathology, Penang General Hospital) and Dato Dr Norain Binti Karim (Head of Department, Department of Pathology, Hospital Raja Permaisuri Bainun Ipoh) for their permissions to collect histopathological samples from their laboratories. Special thanks also to my microbiologist from Penang General Hospital, Ms Keah Kwee Choo, who has been very supportive to me, being constantly alerting me on new culture-proven human melioidosis cases as and whenever available.

I would also like to express my heartfelt gratitude to the masters and PhD students from the developmental laboratory for being friendly and helpful, especially Lin Chuan and Soon Hao who had sacrificed their valuable time assisting me in all the technical aspects of the study.

CONTENTS **Page Number**

ABSTRACT

Melioidosis is not commonly encountered in diagnostic surgical pathology. However it is still an important entity to be recognized due to its high mortality and morbidity rates. In this study, we described the general and specific light microscopic features of melioidosis observed in 27 human melioidosis cases, and assessed the usefulness of *in situ hybridization* (ISH) in the diagnosis of melioidosis in surgical pathological specimens. We applied a nonfluorescent, colorimetric ISH assay using a specific DNA probe to target the 16s ribosomal RNA of *Burkholderia pseudomallei* in formalin-fixed, paraffin-embedded, surgical pathology specimens from known cases of melioidosis and other infected human tissues. Light microscopy revealed that apart from acute, chronic, mixed or granulomatous inflammation, cell-to-cell fusion leading to multinucleated 'giant cell' formation appeared to be a helpful diagnostic clue to severe acute melioidosis. As for ISH, three out of twenty seven cases showed positive reactions, in which intact bacilli, both intra- and extracellular were stained strongly within the inflammatory lesions. Although the sensitivity was not as good as bacterial culture, ISH appeared to be a potentially useful diagnostic tool, especially in the setting where fresh tissue/material was not available for culture studies.

INTRODUCTION

Melioidosis is a potentially fatal infection caused by a gram-negative facultative intracellular bacterium and soil saprophyte, *Burkholderia pseudomallei*. Melioidosis is endemic to Southeast Asia and northern Australia. In Malaysia, cases are continuously being reported. However, the true incidence of infection is still unknown as it is not notifiable under the Prevention and Control of Communicable Diseases Act 1988 (Act 342)[1].

Melioidosis can affect any part of the body. The clinical presentation is variable, ranging from severe community-acquired pneumonia, septicaemia, abscess formation in various organs, septic arthritis and skin lesions. In addition, there is also the quiescent/latent form of infection that may take several years to become symptomatic. Relapsing and recurrent infections are not uncommon, especially in those who are immunocompromised, and can occur in spite of appropriate and prolonged antimicrobial therapy[2].

It has long been recognised that *B. pseudomallei* is an opportunistic pathogen. Although in endemic countries, the exposure to the organism may be widespread, disease manifestation is not common; occurring predominantly in those with underlying predisposing conditions suggesting that the host susceptibility is an important factor. In Malaysia, diabetes mellitus is the most frequently reported predisposing condition. Other predisposing conditions include chronic renal disease, AIDS, malignancy, steroid therapy, alcoholism, occupational exposure, trauma and parenteral drug abuse[4].

Mortality due to melioidosis can be extremely high, especially the septicaemic form, as was shown in a local study in Pahang[3]. The overall mortality of septicaemic

melioidosis approaches 100% (91.8%) if untreated, but can be reduced to 37-54% with optimal management and aggressive intensive care. This again stresses the importance of early, accurate diagnosis and timely treatment. Localised melioidosis has a much lower mortality rate (4-5%), but precise diagnosis is still necessary to enable appropriate treatment for pathogen eradication, and prevention of relapse or recurrence.

Melioidosis is difficult to distinguish from a number of other diseases on clinical grounds alone. A high index of suspicion and history of possible exposure therefore is paramount to aid clinical diagnosis and laboratory tests are essential to confirm the diagnosis. To date, there is no inexpensive, practical, accurate and rapid commercially-available diagnostic test. Diagnosis is still largely based on culture of the organism, which requires prolonged incubation and laborious biochemical methods such as the API 20NE for confirmation[13]. Molecular techniques using conventional, multiplex, or real-time PCR [9-11]and DNA[12] microarrays have greatly improved the speed of diagnosis. However, these newer techniques are expensive, not readily available and may suffer from easy contamination leading to false positive results. In the absence of clinical specimens for culture, serological test may be helpful. However, this method has been hampered by several factors, which includes raised antibody levels in the healthy population in endemic areas[5], presence of subclinical and asymptomatic infections and poorly standardized antigens and probable cross reaction with other *pseudomonas* species[6].

Histopathological examination using routine haematoxylin and eosin (H&E) stain alone often shows inflammatory lesions that appear no different from acute or chronic inflammation due to other causes. These lesions are either an acute-on-chronic inflammation with a focal granulomatous component, or purely

granulomatous in character. Most of the time, diagnosis cannot be confidently made, although the presence of numerous intracellular bacteria within the macrophages forming 'globi' and multinucleated 'giant cells' in a background of acute necrotizing inflammation have been suggested as useful diagnostic clues in acute septicaemic melioidosis[7]. These characteristic 'giant cells' resembled neither Langhans' nor foreign body-type multinucleated giant cells. The cellular origin and mechanism by which they were formed are unclear. The initial suggestion was that these could possibly represent giant macrophages with phagocytosed leucocytes[7]. More recently, Kespichayawattana et al[18] had successfully demonstrated the ability of *B. pseudomallei* to survive inside phagocytic and non-phagocytic cells and induce in vitro cell-to-cell fusion, which was believed to be directly responsible for the multinucleated 'giant cell' formation.

Demonstration of *B. Pseudomallei,* the gram-negative bacteria in formalin-fixed, paraffin-embedded sections are generally difficult even with the help of Gram stain[7]. Immunohistochemical technique using *B. pseudomallei*-specific antibodies has also been studied, but difficulties in visualizing the individually stained bacteria had been observed, and there is often a high background of positively-stained bacterial debris[8].

Recently, *in situ* hybridization (ISH), a molecular assay that uses labelled probes to hybridize with nucleotide targets has been adapted by Eu et al[13] for the identification of *Burkholderia* bacteria in formalin-fixed, paraffin-embedded infected human autopsy tissue and experimentally-infected mouse tissues. A DNA probe that targets the 16s ribosomal RNA of *B. pseudomallei* (Fig 1) and uses a non-fluorescent, colorimetric detection method was developed. It was found to be useful and sensitive enough to stain whole bacilli to facilitate localization and identification

in infected tissues. Compared to the fluorescent ISH technique described by Hagen et al[14], the colorimetric ISH technique appears to be superior as it facilitates light microscopic assessment of the surrounding tissues in which the bacteria were found without the problems of poor background details, auto fluorescence and signal fading. Detection of other pathogens (such as *Helicobacter pylori, Haemophilus influenzae* and *Klebsiella pneumonia)* by ISH method had also been proven to be successful in various types of clinical specimens [32, 33, 34].

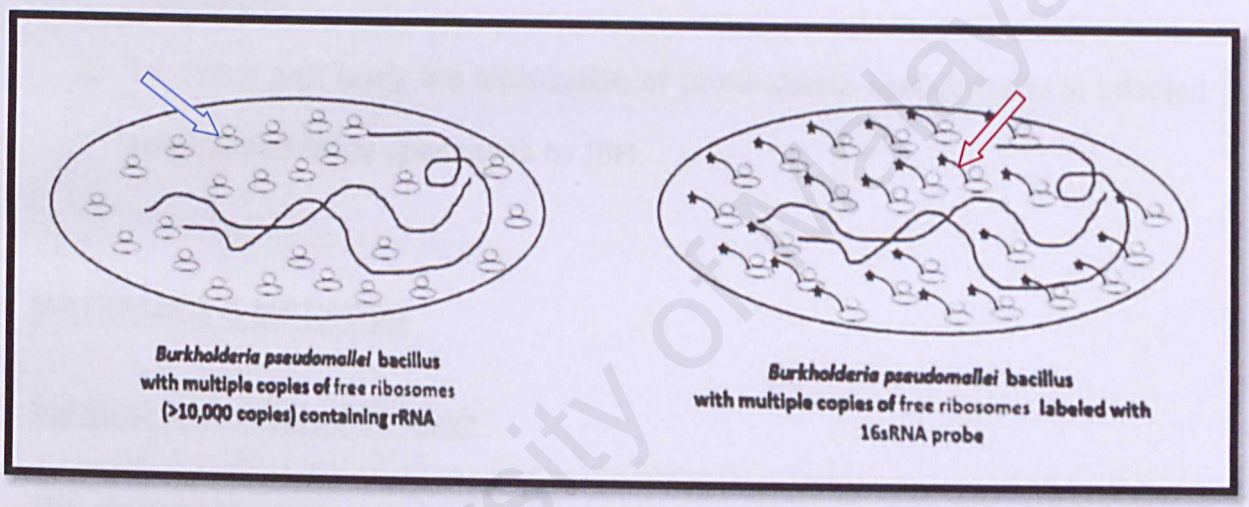

Figure 1: Diagrams showing hybridization of labeled probes (red arrow) to B. pseudomallei 16s rRNA found within free ribosomes (blue arrow), before and after ISH.

OBJECTIVES

General Objectives

To study the infectious disease pathology of melioidosis and to assess the usefulness of ISH assay in its diagnosis.

Specific Objectives

1. To describe general and specific light microscopic features of inflammation in melioidosis
2. To detect and study the localization of *Burkholderia pseudomallei* in infected surgical pathology specimens by ISH.

MATERIALS & METHODS

Surgical pathology specimens

The study included 27 culture-proven cases and 1 PCR/DNA sequencing confirmed case of human melioidosis, in which suitable histopathological tissues were available for study. Nineteen cases were recovered from the archives of the Department of Pathology, Hospital Pulau Pinang (HPP) (Year 2008-2016), six cases from the Department of Pathology, Hospital Raja Permaisuri Bainun Ipoh (HRPBI) (Year 2010-2015), a case from the Department of Pathology, Hospital Sultanah Aminah Johor Bahru (HSAJB) (Year 2011) and a case from the University Malaya Medical Centre (UMMC) (Year 2011). All the tissues were formalin-fixed and routinely processed for paraffin-embedding.

Clinical summaries of the cases were retrieved from the histopathological examination request forms. All the available archival H&E slides were collected from the respective laboratories for review of histopathological features. For those cases with no H&E slides available or faded H&E slides, tissue sections (3 micron thick) were cut from the available tissue blocks and stained with haematoxylin and eosin following routine protocols.

ISH protocol

Tissue sections, 3 micron thick, were cut from the tissue blocks, subsequently deparaffinised, rehydrated and subjected to the *in situ* hybridization procedure. The *in situ* hybridization technique was performed according to the protocol described by Eu et al[14]. First, the deparaffinised and rehydrated 3 micron tissue sections were pre-treated sequentially with 0.2N HCl (20 min, room temperature), proteinase-K (100 μg, 20 min, 37 °C), and lysozyme (1 mg/ml, 30 min, room temperature). The sections were then incubated overnight at 42 °C in standard hybridization buffer (Appendix 3) together with ~1 ng/ml of DIG-labelled DNA probes. After the washing and blocking steps, anti-digoxigenin antibody (Roche, Germany) conjugated with alkaline phosphatase was added followed by the Liquid Permanent Red (Dako, USA) as substrate. Finally, the tissues were counterstained with Mayer's haematoxylin, mounted with Faramount (Dako, USA) and systematically viewed under light microscopy.

Formalin-fixed, paraffin-embedded experimentally-infected mouse tissues (prepared as according to Eu et al[14]) were adopted as positive controls. Normal human and mouse tissues (one each), as well as human tissues known to be infected by fungal

organisms (five), *Mycobacterium tuberculosis* (one), *Mycobacterium leprae* (one) and *Actinomyces spp.* (one) were used as negative controls.

Immunohistochemistry staining procedure

Additional immunohistochemical stains were performed on the acute severe melioidosis case with 'giant cell' formation (Case 3) in an attempt to determine the cellular origin of the 'giant cells'. These includes CD15 (Dako, Carb-3), CD68 (Dako, PG-M1), CD61 (Thermo Scientific, 2f2) and Cytokeratin AE1/AE3 (Dako, AE1/AE3). The staining method for IHC was performed on formalin-fixed, paraffin-embedded tissue sections. Preparation of tissues, slides, immunohistochemical procedure, preparation of controls and determination of positivity and negativity of the staining were done according to the manufacturing company standards and guidelines.

Flow chart of study methodology

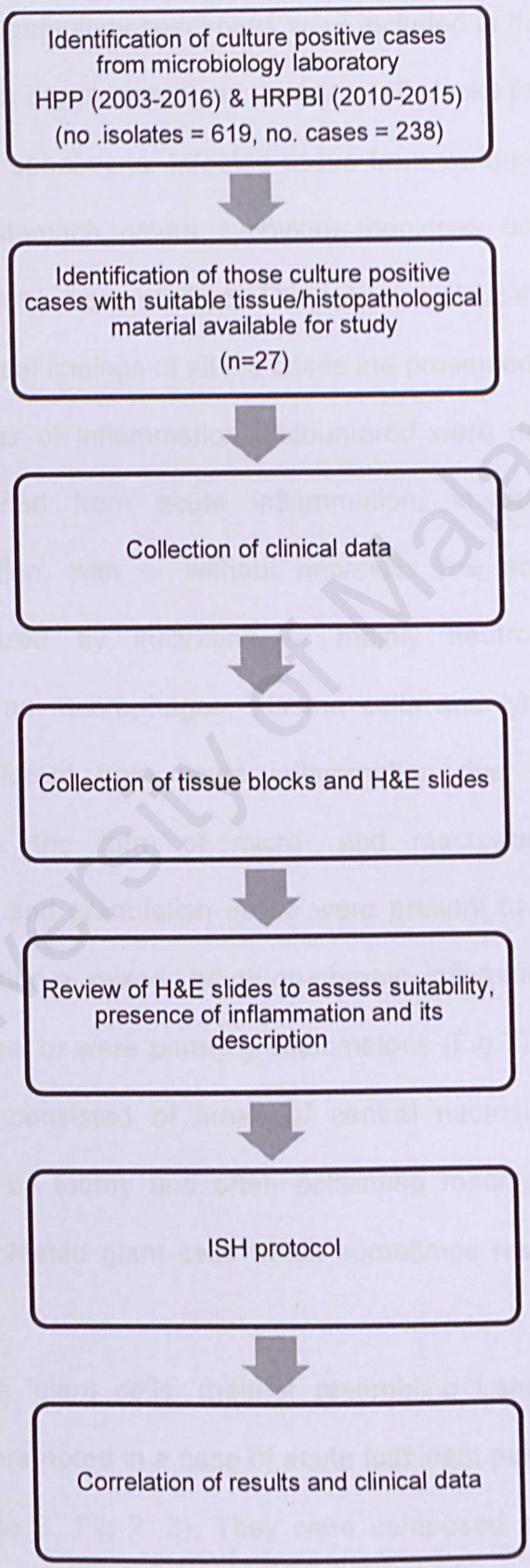

RESULTS

1. Review of H&E slides

A variety of surgical pathology specimens were included in this study, ranging from small biopsies to larger organ resections, and two cell blocks prepared from fine needle aspiration cytology specimens. Infected tissue from various organs such as lung, spleen, liver, testis, stomach, pleura, synovium, meninges, bone, skin and soft tissue from various locations were studied. The relevant clinical information and summary of histopathological findings of all the cases are presented in Table 1.

Generally, the types of inflammation encountered were neither tissue- nor organ specific, and varied from acute inflammation, abscesses to chronic granulomatous inflammation, with or without necrosis. The acute inflammatory lesions were characterized by infiltration of mainly neutrophils and other inflammatory cells such as macrophages, plasma cells and lymphocytes, which appeared to be no different from acute inflammation due to other causes. Inflammation often took the form of micro- and macroabscesses (Fig 6). Hemorrhage, congestion and granulation tissue were present to a variable extent. Many of them show either a mixed, acute-on-chronic inflammation with a focal granulomatous component, or were purely granulomatous (Fig 7) in nature. In most cases, the granulomas consisted of areas of central necrosis with or without neutrophils, surrounded by foamy and often palisading macrophages, epithelioid cells and a few multinucleated giant cells which sometimes resembled Langhan's giant cells (Fig 9: E,F).

The characteristic 'giant cells' (neither resembling Langhan's nor foreign body-type giant cells) were noted in a case of acute fulminant pulmonary melioidosis with fatal outcome (Case 3, Fig 2, 3). They were composed of multiple smudgy,

degenerated-looking nuclei that clumped together and sharing a rounded, distinct to ill-defined cytoplasmic borders (Fig 4). They were seen scattered within the necrotic areas in the lung abscesses. Additional finding observed in this case was the presence of fibrin thrombi within the branches of pulmonary arteries (Fig 5), which may suggest the presence of complications such as disseminated intravascular coagulopathy in this patient. Representative pictures of all the cases are shown in Appendix 1.

Table 1: Demography, clinical and histopathological features of 27 known melioidosis cases

Case no.	Sex/ Age	Clinical features and diagnosis	Positive culture obtained from	Histopathological features
1	M/36	History of medullary thyroid carcinoma and pheochromocytoma, presented with slurring of speech and headache	tissue, swab	**Dura and brain tissue (biopsy):** Suppurative and necrotizing granulomatous inflammation. Occasional multinucleated giant cells and a few thickened wall and necrotic blood vessels are noted.
2	M/25	Presented with liver abscess and pneumonia, treated as systemic melioidosis.	blood, tissue, pus, tracheal aspirate, swab	**Liver (segmental resection):** Multiple foci of necrosis surrounded by mixed but mostly chronic inflammatory cells composed of macrophages, lymphocytes, plasma cells and some neutrophils.
3	M/ 48	Known case of diabetes mellitus, hypertension, history of stroke and end stage renal failure with renal transplant done in 2009 (on immunosuppressant), presented with cough and fever for 3 weeks, rapidly deteriorated into septic shock. Treated as systemic melioidosis with lung and splenic involvement. Left lung upper lobectomy was performed. Patient passed away in immediate postoperative period.	blood, tissue, tracheal aspirate	**Lung (lobectomy):** Multiple discrete and coalescing abscesses with destruction of alveolar wall. Scattered 'giant cells' with distinct rounded to ill-defined cell borders and multiple smudgy, degenerated looking nuclei are seen. Fibrin thrombi are noted within the branches of pulmonary arteries, away from the inflammatory lesions.
4	F/44	Known case of diabetes mellitus on insulin with history of right knee septic arthritis, presented with right below knee subcutaneous abscess. Incision and drainage was performed. Abdominal ultrasound showed no visceral abscess.	tissue	**Synovium (biopsy):** Fibrogranulation tissue mildly infiltrated by mixed acute and chronic inflammatory cells, with focal non-necrotizing granulomatous inflammation and occasional multinucleated giant cells.
5	M/73	Known case of hypertension, presented with right septic arthritis.	tissue, blood	**Synovium (biopsy):** Suppurative and necrotizing inflammation. No granuloma or giant cell.
6	F/30	History of left gluteal abscess with incision and drainage done. Subsequently presented with non-healing surgical wound and gluteal sinus.	tissue	**Gluteal tissue (biopsy):** Suppurative inflammation. No granuloma or giant cell.
7	F/31	Known case of diabetes mellitus and bronchial asthma, presented with liver and splenic abscesses. Treated with IV Ceftazidime and Amphotericin prior to splenectomy.	pus, blood, tissue	**Spleen (splenectomy):** Numerous large neutrophilic abscesses surrounded by haemorrhagic splenic parenchyma. No granuloma or giant cell.

Case no.	Sex/ Age	Clinical features and diagnosis	Positive culture obtained from	Histopathological features
8	M/6	Presented with bilateral exudative tonsillitis, right neck parapharyngeal abscess and multiple enlarged cervical lymph nodes. Abdominal ultrasound showed no visceral abscess.	Pus	**Lymph nodes (excision):** Partial or near complete nodal architectural effacement by suppurative and necrotizing inflammation forming abscesses. No well-formed granuloma or giant cell.
9	M/28	Ex-IVDU, known to have history of pulmonary tuberculosis and diabetes mellitus, presented with right lung empyema. Treated with IV Ceftazidime and Fluconazole.	pleural fluid, swab	**Pleura (biopsy):** Fibrogranulation tissue focally covered with fibrinosuppurative exudates. No granuloma or giant cell.
10	F/47	Newly diagnosed diabetes mellitus, presented with diabetic ketoacidosis, varicella zoster with pneumonitis, liver and splenic abscesses. Treated as melioidosis.	blood	**Spleen (splenectomy):** Multiple abscesses within the parenchyma and subcapsular region. The edge of the abscesses shows epithelioid macrophages, lymphocytes, plasma cells and occasional multinucleated giant cells.
11	M/26	Known case of diabetes mellitus and had history of suspected and empirically-treated pulmonary tuberculosis, presented with left lung empyema.	pleural fluid	**Pleura (biopsy):** Fibrogranulation tissue showing focal dense mixed acute and chronic inflammatory cells infiltration. No granuloma or giant cell.
12	M/27	Presented with splenic abscess. Treated as melioidosis, on IV Imipanem, Doxycyclin, Bactrim and Chloramphenicol.	blood	**Spleen (splenectomy):** Extensive areas of haemorrhage and necrosis surrounded by some histiocytes, lymphocytes and neutrophils. No well-formed granuloma or giant cell.
13	M/59	Known case of diabetes mellitus and hypertension, presented with left testicular abscess. Treated with IV Ceftazidime.	swab	**Testis (orchidectomy):** Haemorrhagic and extensively necrotic testicular parenchyma with very minimal residual viable seminiferous tubules. Neutrophilic abscesses and dense infiltrates of mixed acute and chronic inflammatory cells are present. No granuloma or giant cell.
14	M/56	Presented with liver and splenic abscesses. Treated as melioidosis and started on IV Ceftazidime. Also noted right parotid swelling likely abscess formation. Fine needle aspiration of right parotid swelling done and cell block performed.	blood, pus	**Cytology smear:** Moderate cellularity smears showing predominantly neutrophils with some degenerated cells and histiocytes. Occasional clusters of epithelial cells are seen. No granuloma or giant cell. **Cell block:** Poor cellularity; Mainly fibrin and small aggregates of neutrophils.

Case no.	Sex/ Age	Clinical features and diagnosis	Positive culture obtained from	Histopathological features
15	M/51	Known case of diabetes mellitus, presented with chronic cough for 3 months. CT scan shows right upper lobe mass with cavitation. Sputum AFB repetitively negative. CT guided-lung biopsy done.	blood	**Lung (biopsy):** Necrotizing granulomatous inflammation with multinucleated giant cells resembles Langhan's type, morphologically highly suspicious of tuberculosis.
16	F/50	Presented with right knee septic arthritis. Treated with IV Ceftazidime. Arthrotomy and washout done. Synovial fluid sent for cytology and cell block preparation.	blood	**Cytology smear and cell block:** Abundant neutrophils admixed with some lymphocytes and macrophages. No granuloma or giant cell.
17	M/72	Presented with scalp abscess and occipital and parietal bone osteomyeliltis.	Pus	**Scalp tissue (biopsy):** Fibrogranulation tissue with neutrophilic microabscesses. No granuloma or giant cell. **Bone (biopsy):** Bone with marrow cavity replaced by fibrogranulation tissue. Mild chronic inflammatory cells infiltration seen. No granuloma or giant cell.
18	M/46	Known case of diabetes mellitus on oral hypoglycaemics, presented with cervical spine paravertebral abscess	bone	**Cervical spine (biopsy):** Granulomas with occasional multinucleated giant cells. Small foci of necrosis are seen in some of the granulomas.
19	M/31	Known case of Type 1 diabetes mellitus on insulin with history of left lower back abscess, presented with left thigh abscess	tissue	**Thigh tissue (biopsy):** Suppurative and necrotizing inflammation involving the deep dermis and subcutis. No granuloma or giant cell.
20	F/57	Presented with labial abscess. Treated with IV Ceftazidime.	blood	**Labial tissue (biopsy):** Necrotic tissue fragments with scattered neutrophilic infiltration. No granuloma or giant cell.
21	M/50	Presented with C1-C6 epidural abscess with laminectomy done. Subsequently complicated with infected surgical wound and surgical debridement was done four months later. Treated as melioidosis.	pus	**C1-C6 epidural tissue (biopsy):** Necrotizing granulomatous inflammation with palisading epithelioid macrophages and occasional multinucleated giant cells.
22	M/67	Presented with perforated gastric ulcer, with 2 litres of greenish purulent fluid noted within the abdominal cavity on laparoscopy.	blood	**Stomach (biopsy):** Necrotic tissue admixed with acute inflammatory cells, fibrogranulation tissue and part of muscularis propria. No granuloma or giant cell.

Case no.	Sex/ Age	Clinical features and diagnosis	Positive culture obtained from	Histopathological features
23	M/53	No clinical history provided.	blood	**Bone (biopsy):** Bone, granulation tissue and focal dense neutrophilic infiltration. No granuloma or giant cell.
24	M/48	Carbuncle on the scalp.	blood	**Scalp tissue (biopsy):** Focally ulcerated skin with suppurative and necrotizing inflammation involving the dermis and subcutis. No granuloma or giant cell.
25	M/50	Known case of osteoarthritis and gouty arthritis. Presented with left knee abscess.	blood	**Knee tissue (biopsy):** Acute suppurative and necrotizing inflammation. No granuloma or giant cell.
26	M/19	Newly diagnosed diffuse large B cell lymphoma of small intestine. Bone marrow trephine biopsy was done for staging.	blood	**Bone marrow trephine (biopsy):** Bony trabeculae with the marrow cavity extensively replaced by fibrogranulation and necrotic tissue. Mixed acute and chronic inflammatory infiltrates are seen. No well-formed granuloma or giant cell.
27	M/54	A case of asymptomatic latent melioidosis, incidentally discovered when patient presented with traumatic spleen injury following motor vehicle accident. Patient was known to have diabetes mellitus. The splenectomy specimen was proven to be infected by *Burkholderia pseudomallei* via ISH performed on the tissue sections. This was further confirmed by PCR and DNA sequencing. No initial culture was sent as the infection was not suspected clinically. Subsequently patient developed culture-proven *B. pseudomallei* associated surgical wound infection at Day 4 post-op and multiple superficial abscesses around abdominal scar 16 months later[a].	Pus (from surgical wound infection)	**Spleen (splenectomy):** Coalescing granulomas with central necrosis and peripheral rim of haemorrhage, surrounded by epithelioid macrophages, lymphocytes, occasional neutrophils, and a few multinucleated giant cells, some resembling Langhan's giant cells[a].

[a]Case 27 was previously described by Chow et al.[15]

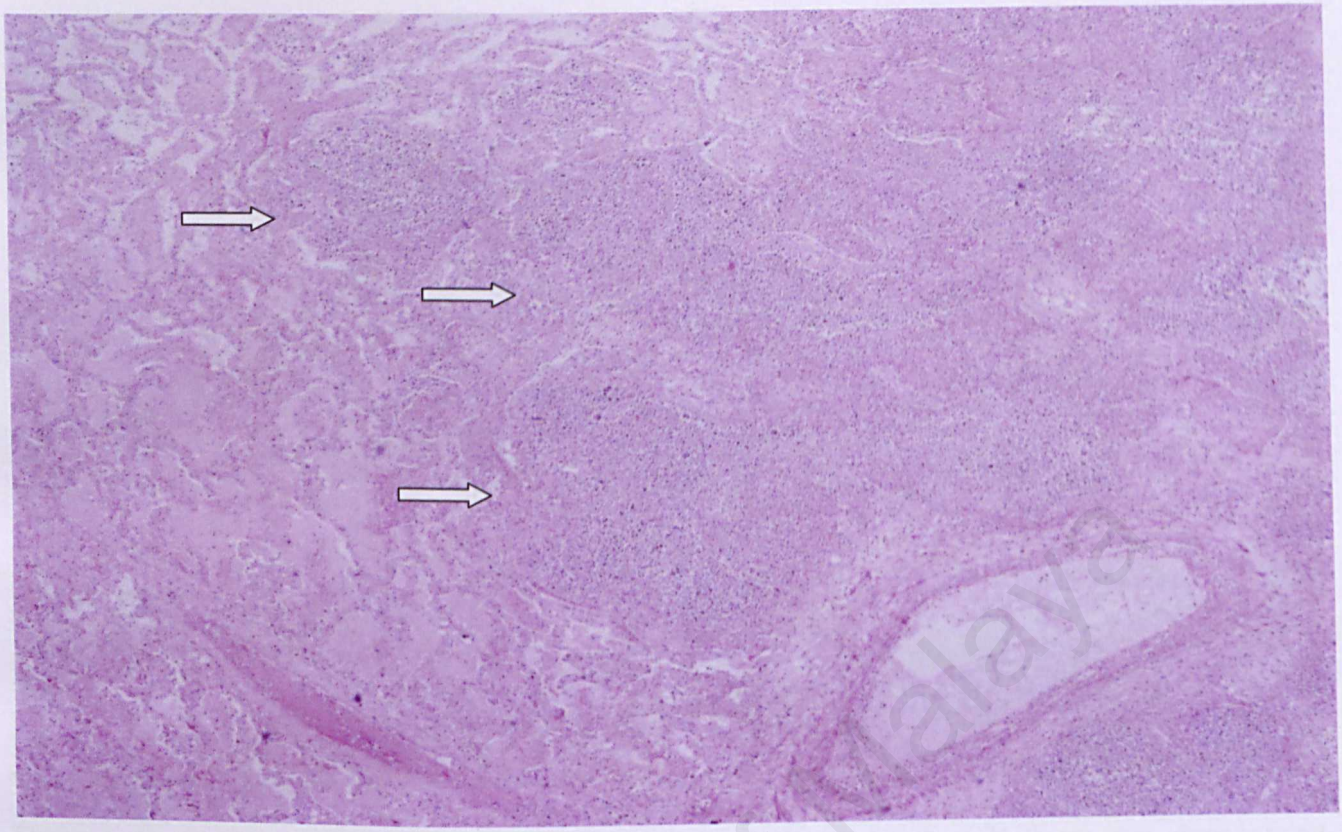

Figure 2: Case 3 [lung]: Acute fulminant pulmonary melioidosis. Multiple discrete and coalescing abscesses (arrow) with destruction of alveolar wall. (H&E; Magnification: 4x objective)

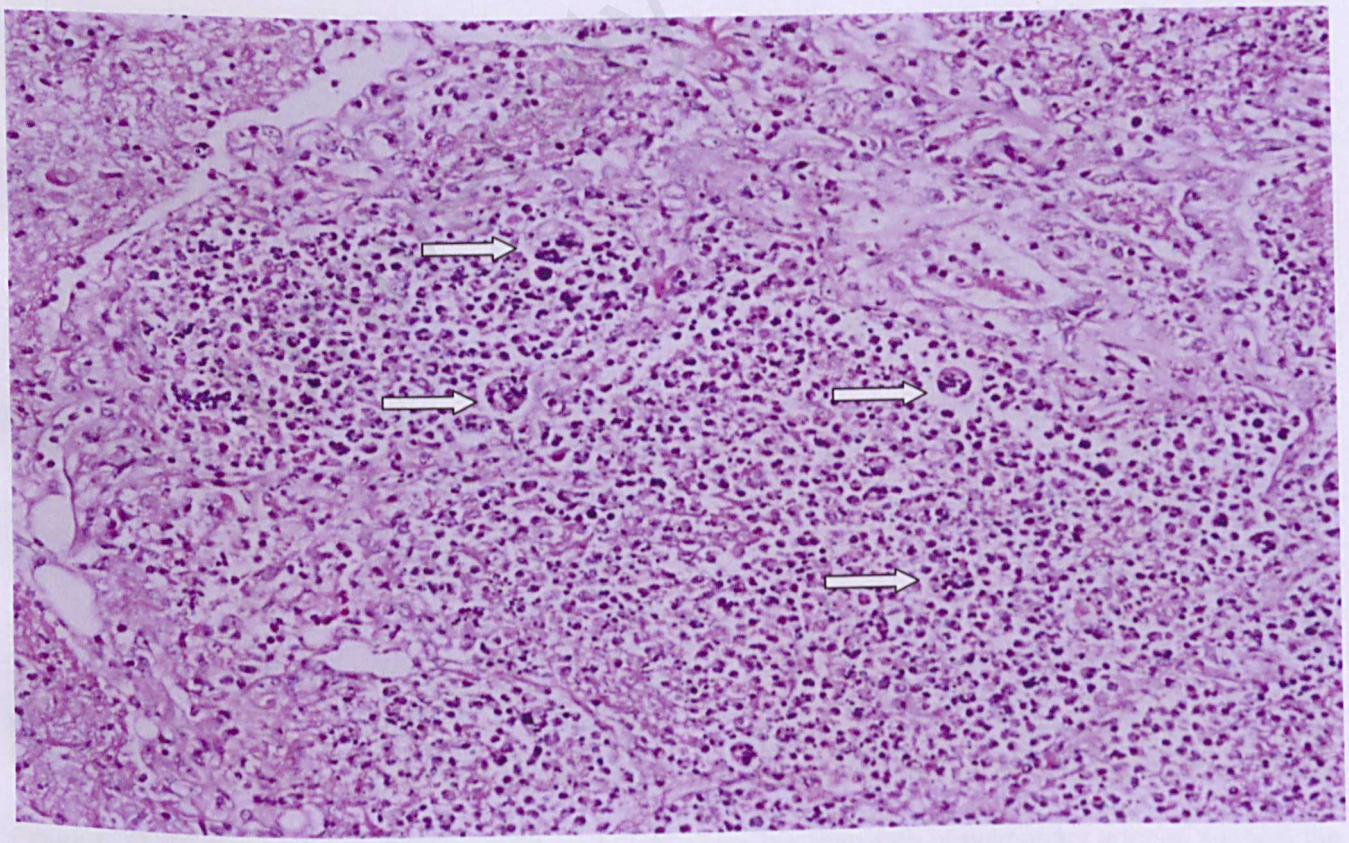

Figure 3: Case 3 [lung]: Acute necrotizing inflammation consisting of neutrophils, macrophages and some scattered 'giant cells' (arrow). (H&E; Magnification: 20x objective)

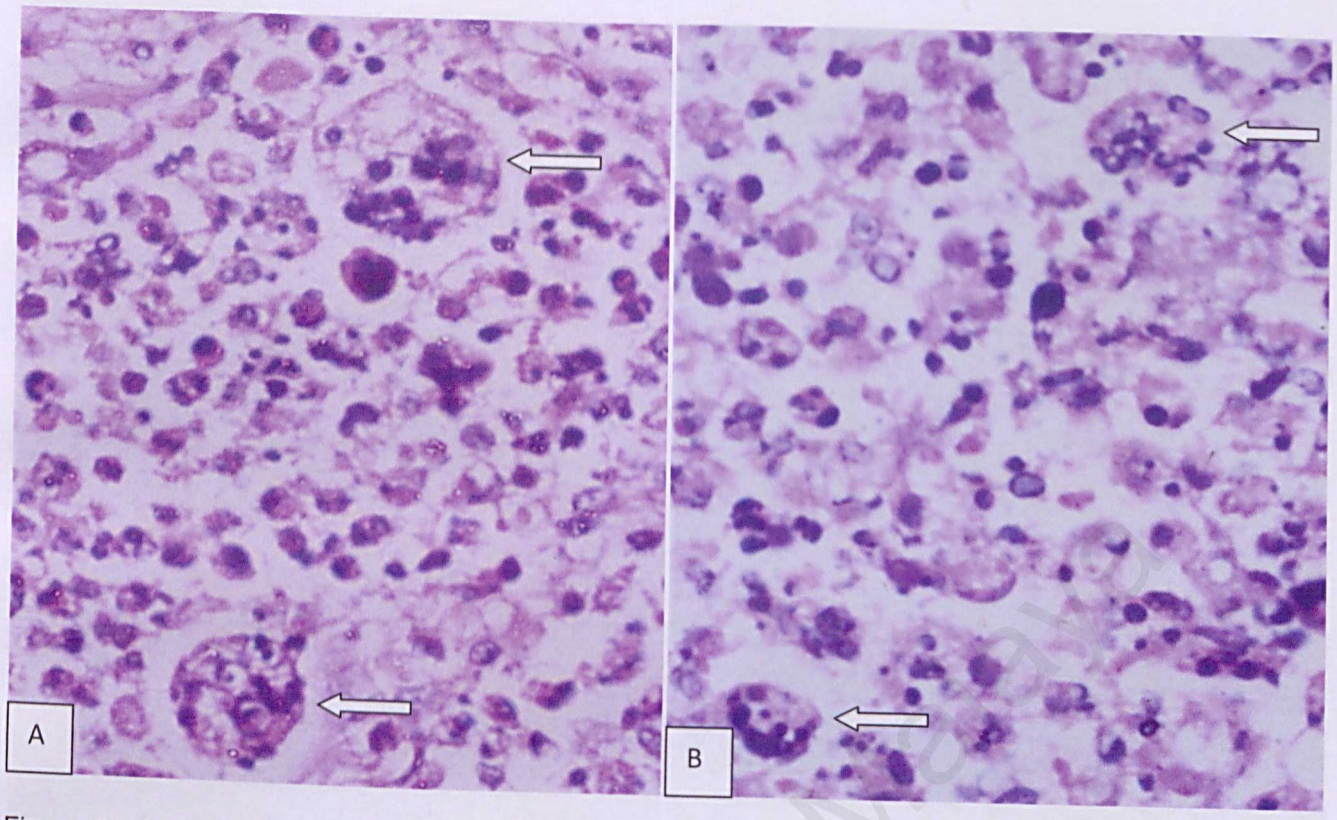

Figure 4: (A, B) Case 3 [lung]: The characteristic 'giant cells' (arrow) with multiple smudgy, degenerated-looking nuclei that clumped together and sharing a rounded, distinct to ill-defined cytoplasmic borders. (H&E; Magnification: A, B: 60x objective)

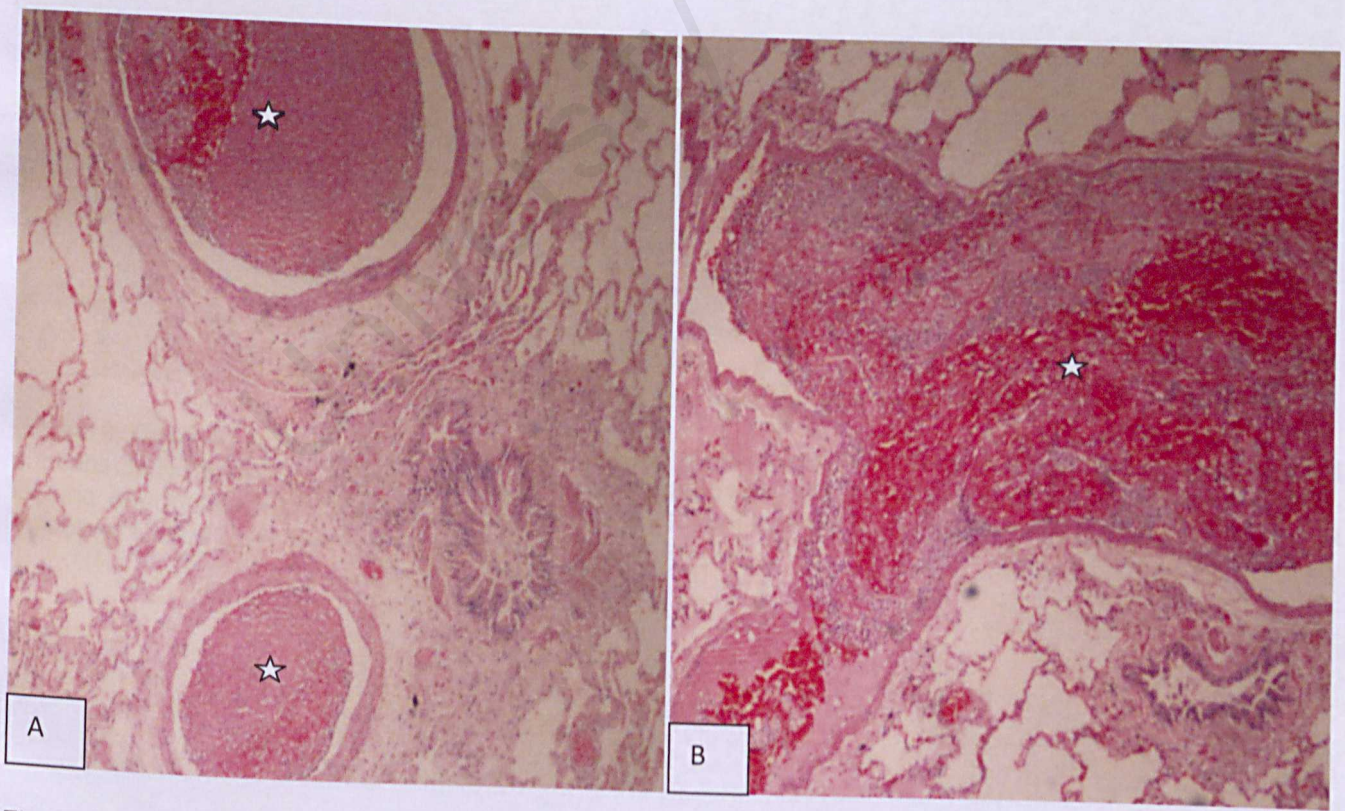

Figure 5: (A, B) Case 3 [lung]: Fibrin microthrombi (☆) within the branches of pulmonary arteries suggest the presence of complications such as disseminated intravascular coagulopathy in this patient (H&E; Magnification: A, B: 4x objective)

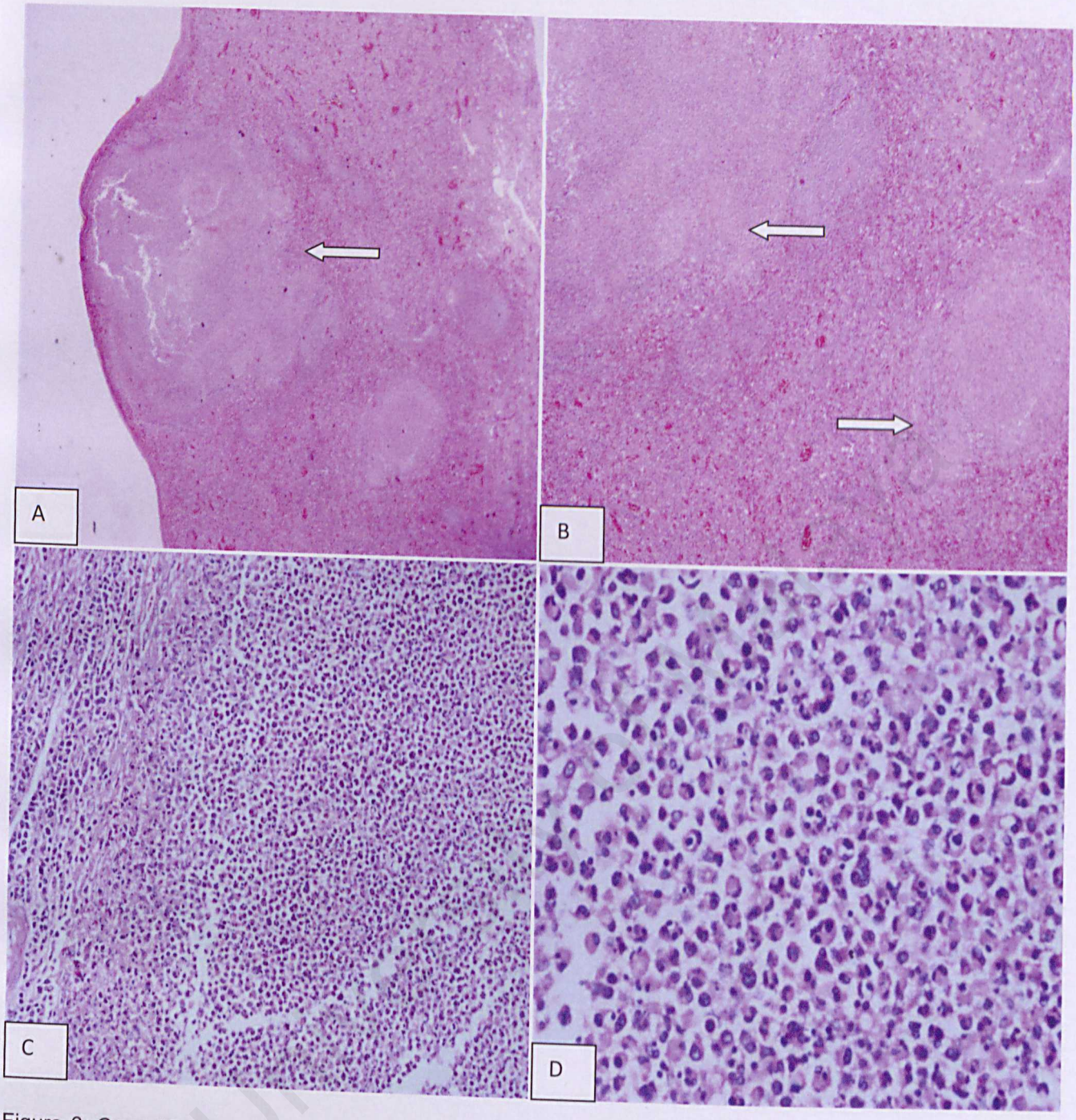

Figure 6: Case 10 [spleen]: (A, B) Congested splenic parenchyma with numerous abscesses, some located subcapsularly (arrow). (C, D) Higher magnification showing dense aggregates of both viable and degenerated-looking neutrophils within the abscess cavity. (H&E; Magnification: A: 2x objective; B: 4x objective; C: 20x objective; D: 60x objective)

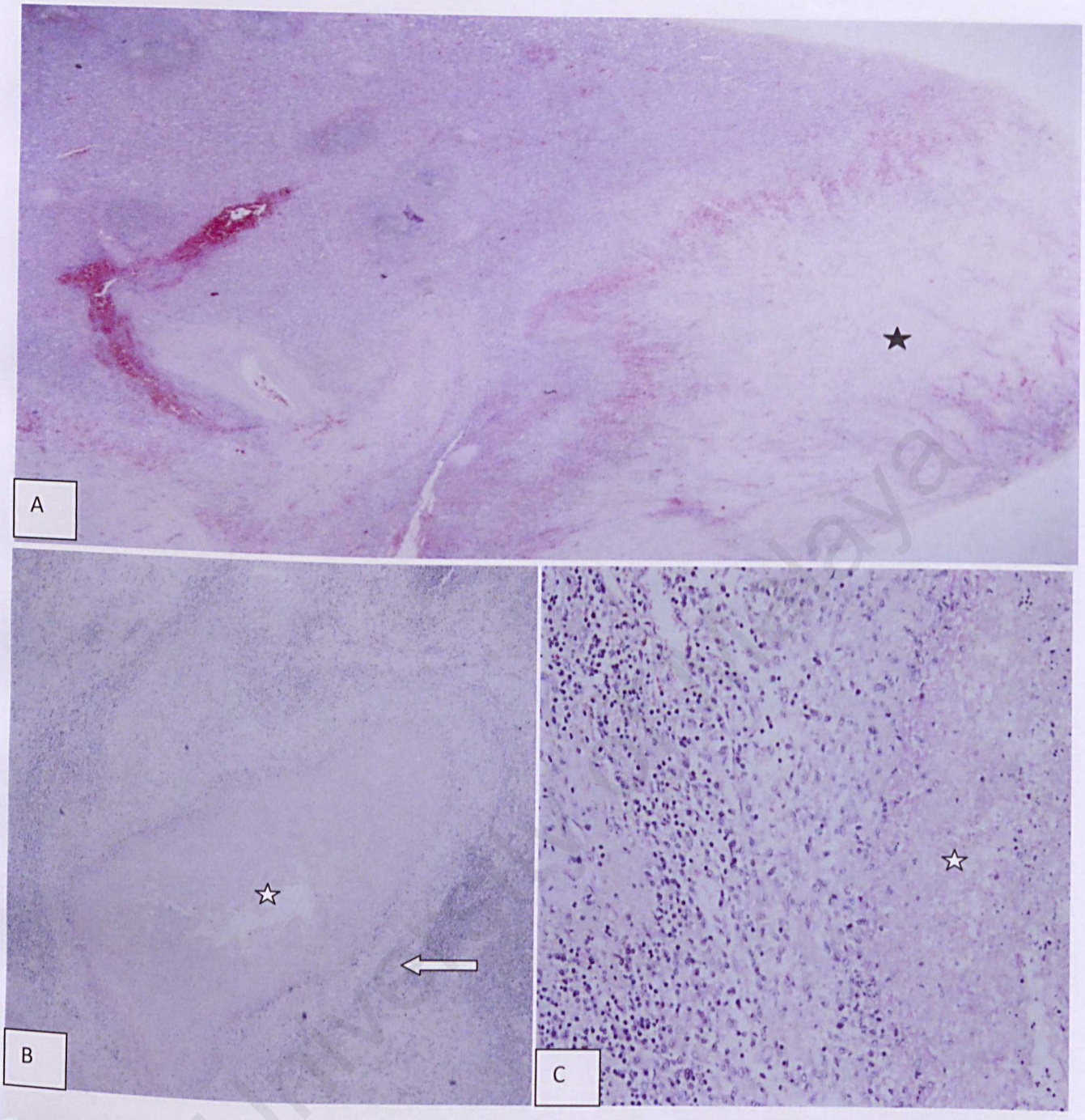

Figure 7: Case 27 [spleen]: Asymptomatic latent melioidosis. (A) Coalescing granulomas (★) with peripheral rim of haemorrhage. (B, C) Higher magnification showing granuloma (arrow) with central necrosis (☆) surrounded by epithelioid macrophages, lymphocytes and occasional neutrophils. (H&E; Magnification: A: 2x objective; B: 4x objective; C: 20x objective)

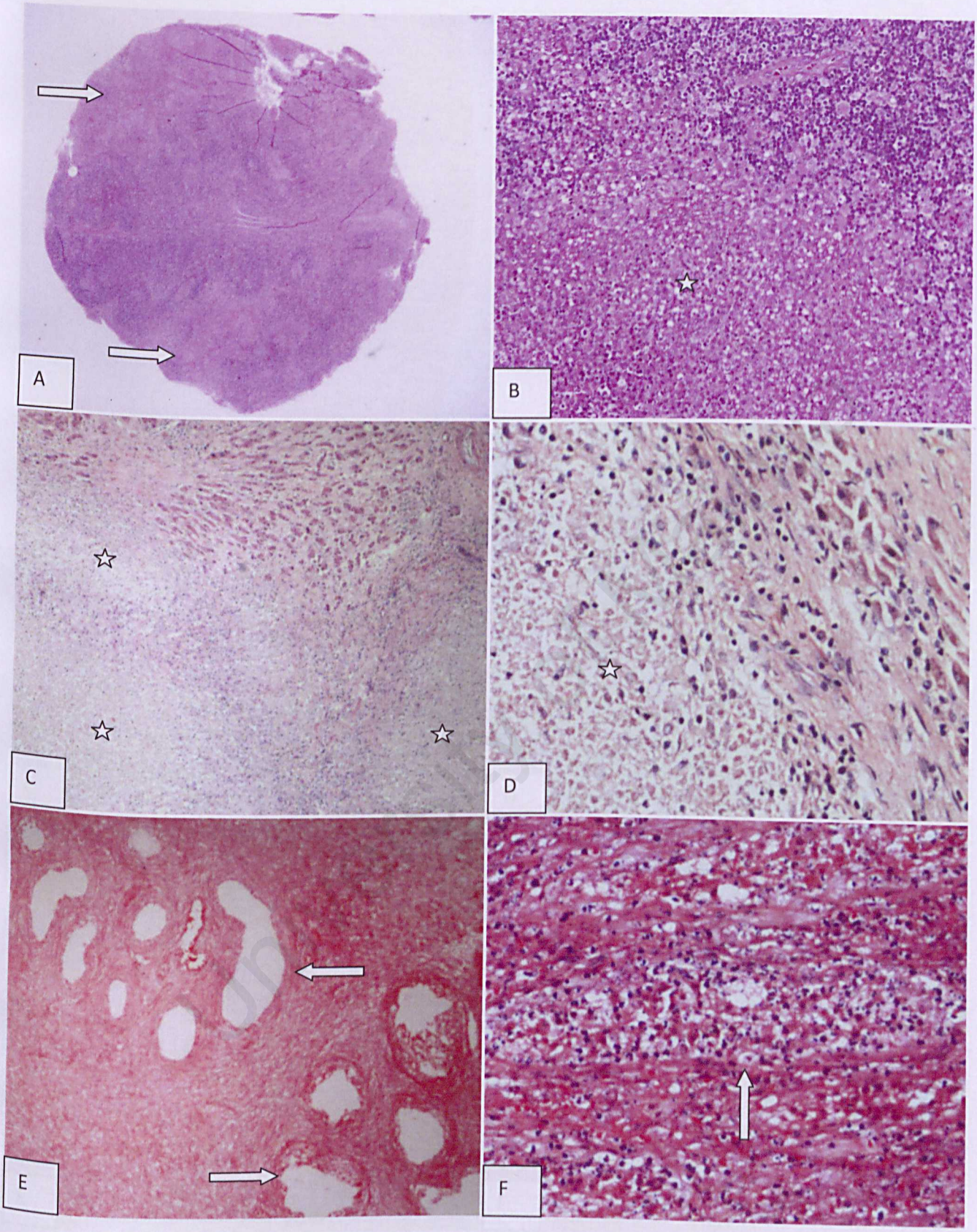

Figure 8: (A, B) Case 8 [lymph node]: Partial nodal architectural effacement by necrotizing and suppurative inflammation (arrow). Residual lymphoid follicles with prominent germinal centres are seen. Higher magnification showing necrotic area (☆) mixed with abundant neutrophils and macrophages. (C, D) Case 2 [Liver]: Multifocal necrosis (☆) surrounded mostly by chronic inflammatory cells. (E, F) Case 13 [testis]: Haemorrhagic and necrotic testicular parenchyma with ghostly outlines of seminiferous tubules (arrow). Some of the seminiferous tubules are densely infiltrated by neutrophils. (H&E; Magnification: A: 2x objective; B: 10x objective; C, E: 4x objective; D, F: 20x objective)

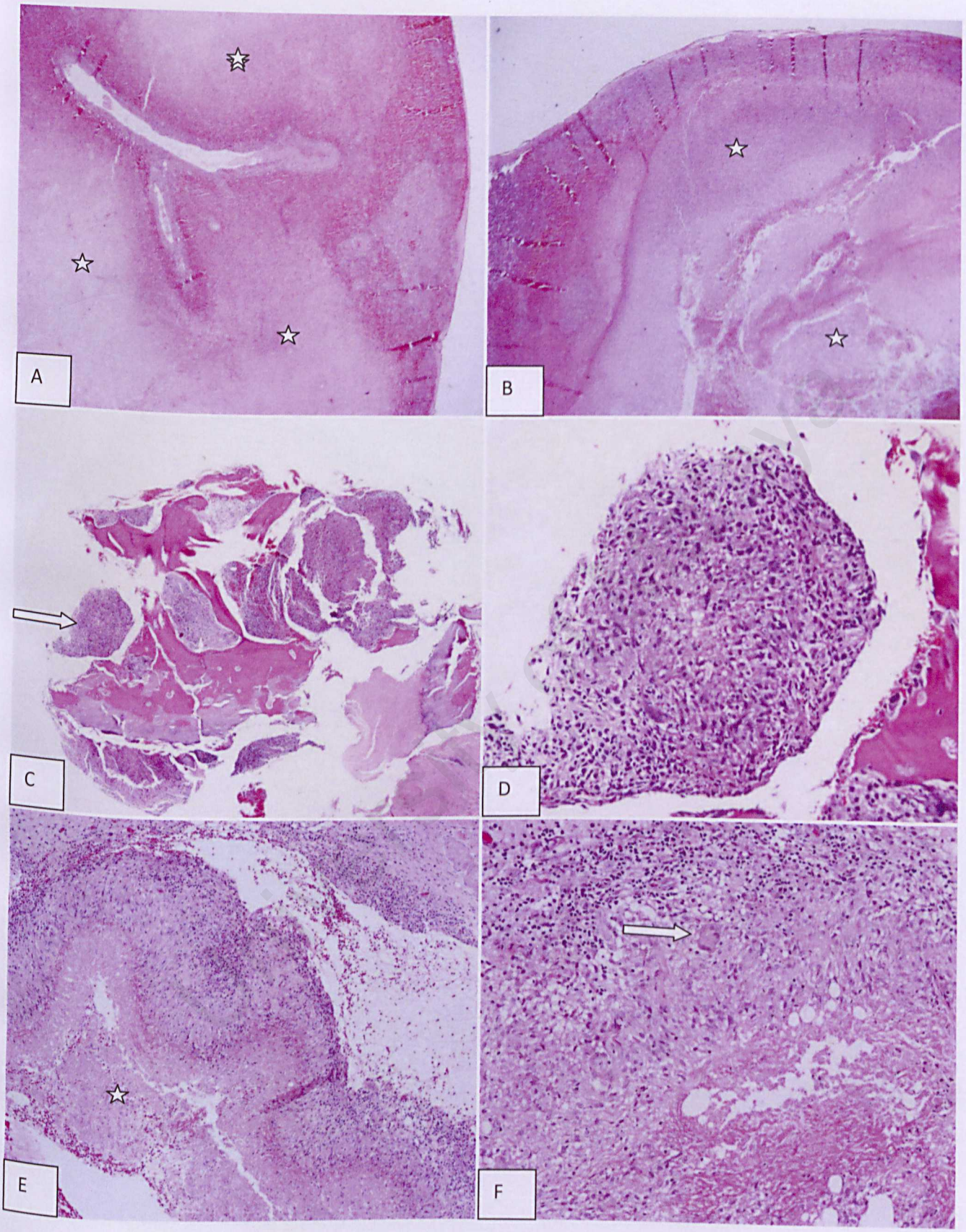

Figure 9: (A, B) Case 7 [spleen]: Numerous large abscesses (☆) surrounded by haemorrhagic splenic parenchyma. (C, D) Case 18 [cervical spine]: Bony trabeculae with the marrow cavity densely infiltrated by mostly chronic inflammatory cells, with a few well-formed granulomas (arrow) seen. (E, F) Case 21 [C1-C6 epidural tissue]: Necrotizing granulomas (☆) with palisading epithelioid macrophages and occasional multinucleated giant cells (arrow) observed. (H&E; Magnification: A, B: 2x objective; C: 4x objective; D, F: 20x objective; E: 10x objective)

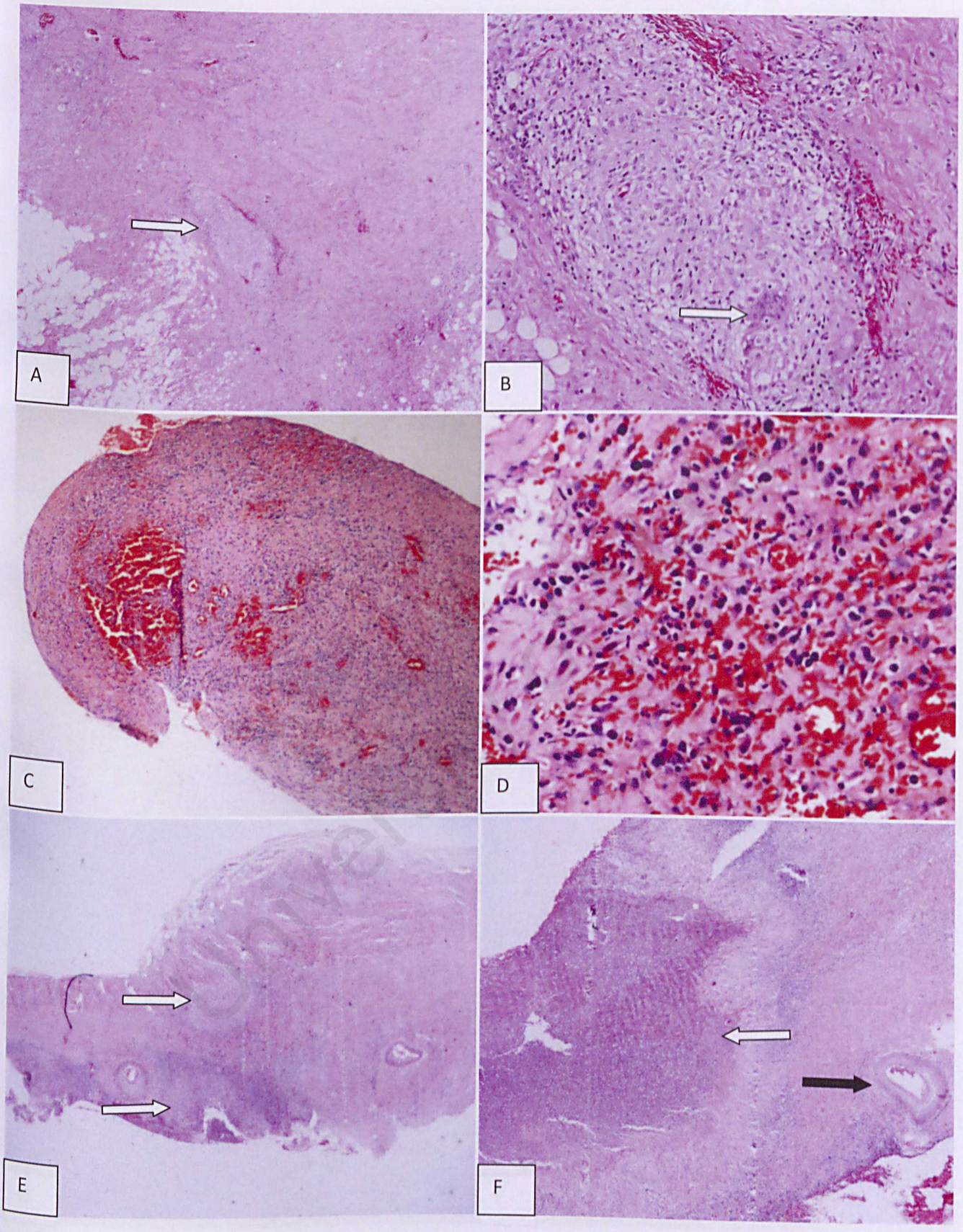

Figure 10: (A, B) Case 4 [Synovium]: Fibrogranulation tissue mildly infiltrated by mixed inflammatory cells, with focal granulomatous inflammation and multinucleated giant cell (arrow). (C, D) Case 11 [pleura]: Fibrogranulation tissue showing dense mixed inflammatory cells infiltration. (E, F) Case 1 [Dura]: Suppurative necrotizing granulomatous inflammation (white arrow) with a few thickened wall and necrotic blood vessels (black arrow). (H&E; Magnification: A, C: 4x objective; B: 20x objective; D: 40x objective, E: 2x objective; F: 10x objective)

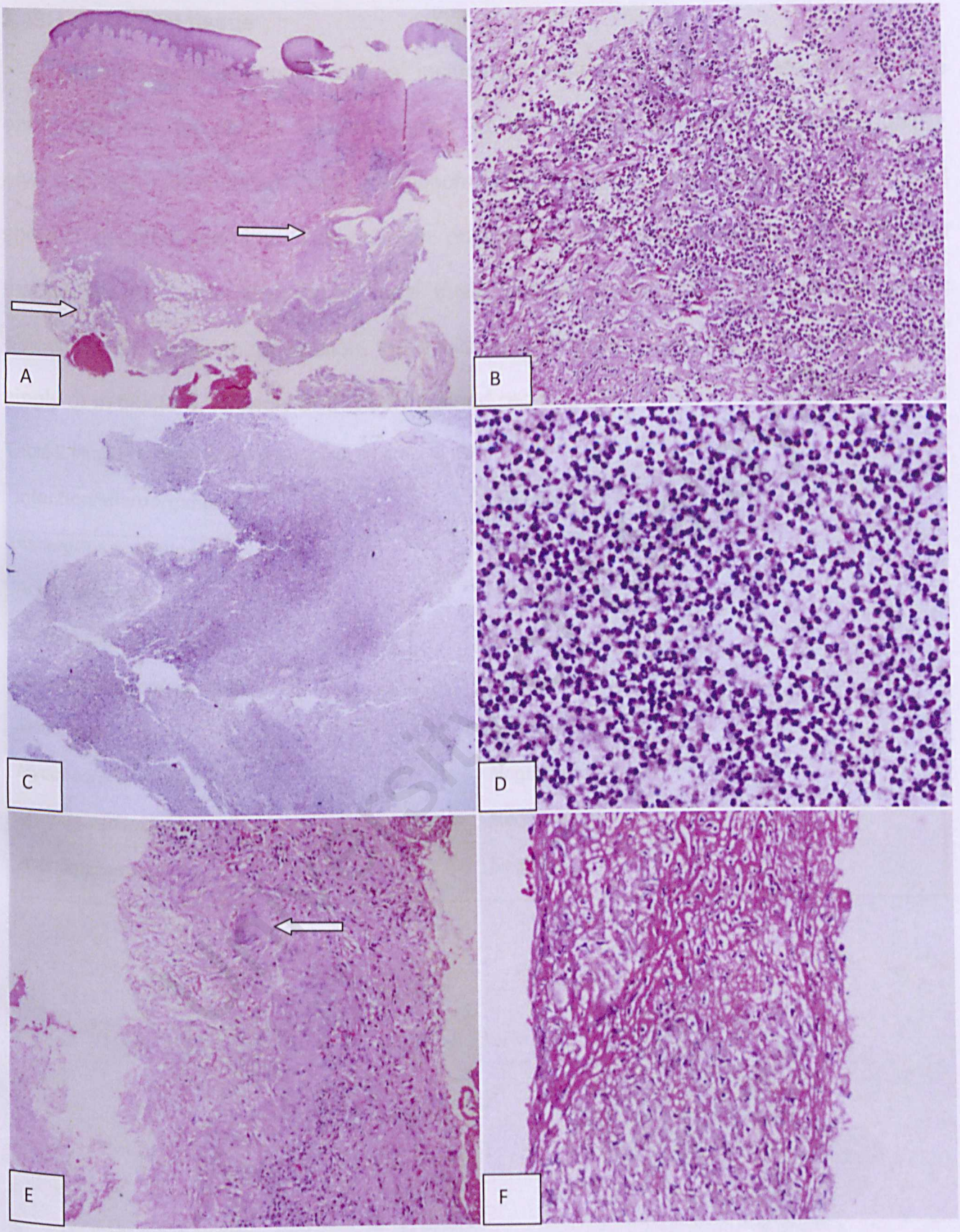

Figure 11: (A, B) Case 19 [thigh tissue]: Suppurative and necrotizing inflammation (arrow) involving mainly deep dermis and subcutis. (C, D) Case 16 [Synovial fluid cell block]: Inflammatory exudates composed predominantly of neutrophils. (E) Case 15 [lung biopsy]: Necrotizing granulomatous inflammation with multinucleated giant cells resembled Langhan's type (arrow). (F) Case 22 [stomach biopsy]: Necrotic cellular debris admixed with mixed inflammatory cells. (H&E; Magnification: A, C: 2x objective; B, E: 20x objective; D,F: 40x objective)

2. ISH on control tissue

All the negative control tissues, including normal human and mouse tissues (one each), as well as human tissues known to be infected by fungal organisms (five), *Mycobacterium tuberculosis (*one*)*, *Mycobacterium leprae* (one) and *Actinomyces spp.* (one) showed negative staining (Table 2). In positive control tissue (experimentally-infected mouse tissue), bacterial colonies were easily spotted under low power (as low as 2x objective). On higher magnification, the bacilli were detected both intra- and extracellularly, singly or in clusters, strongly and crisply stained red (Fig 13).

Table 2 Human tissues used as negative controls in ISH

Infection/Microorganisms	**ISH results**
Aspergillus fumigates	Negative
Acremonium spp	Negative
Histoplasma capsulatum	Negative
Cladophialophora bantiana	Negative
Mucor spp.	Negative
Mycobacterium tuberculosis	Negative
Mycobacterium leprae	Negative
Actinomyces spp	Negative

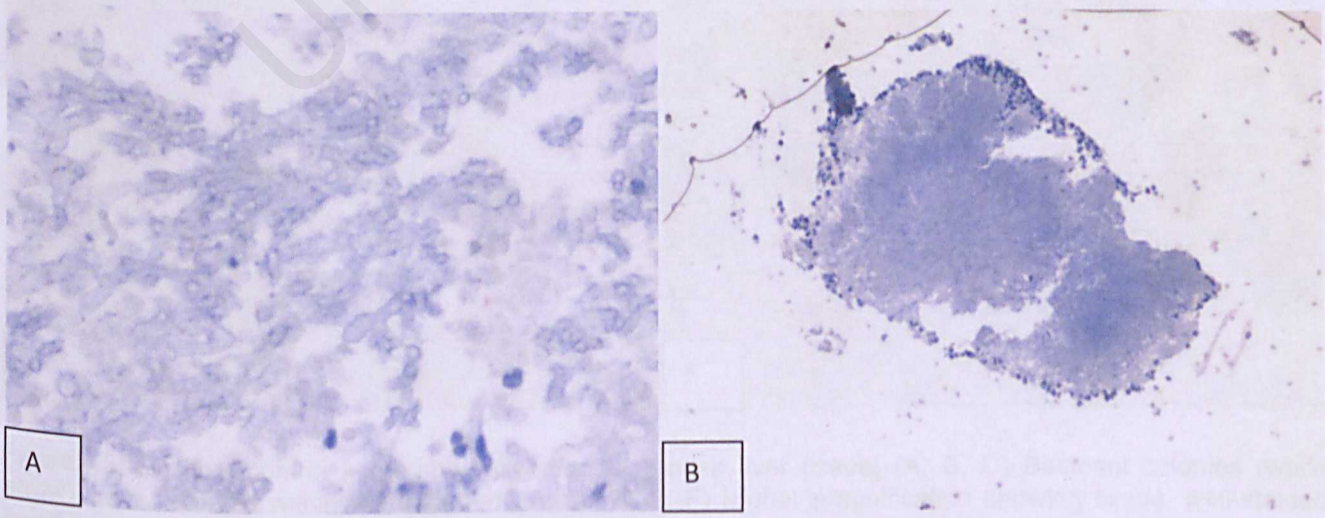

Figure 12: Examples of negative control. A: *Aspergillus fumigatus*; B: *Actinomyces spp.* (ISH/Liquid permanent red; Magnification: A: 40x objective; B: 20x objective)

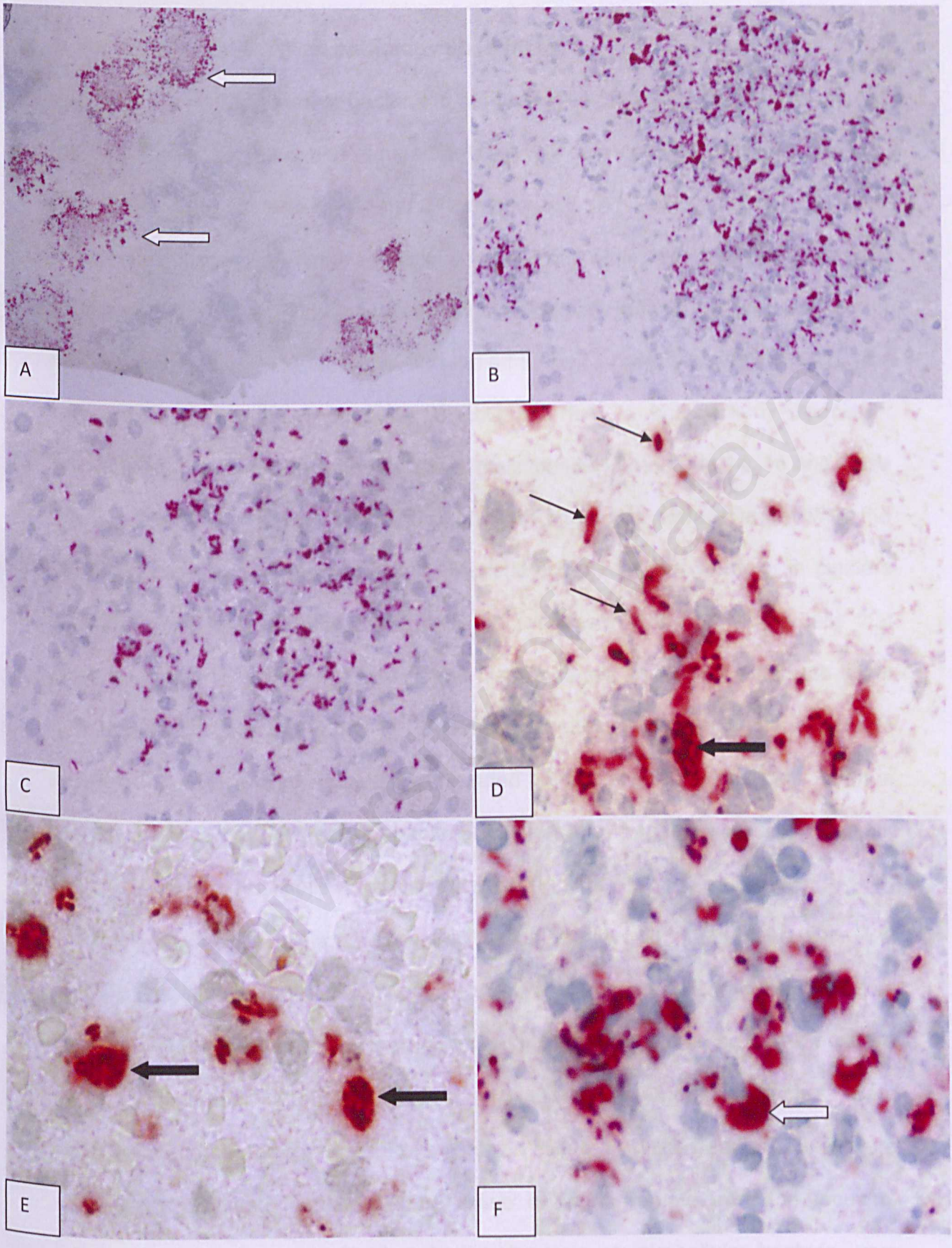

Figure 13: Positive control [experimentally-infected mouse liver tissue] (A, B, C) Bacterial colonies (white arrow) were detected within the inflamed areas. (D, E, F) Higher magnification showing single, well-stained bacillus (thin black arrow) while some in clusters (thick black arrow). Some of these bacilli were clearly seen within the cytoplasm of the inflammatory cells (white arrow). (ISH/Liquid permanent red; Magnification: A: 2x objective; B: 40x objective; C: 60x objective; D, E, F: 100x objective)

3. ISH on infected surgical pathology specimens

Generally, detection of bacteria in surgical cases was difficult as compared to the positive control tissue and required detailed and careful high power examination. Only three cases (Cases 3, 10, and 27) showed patchy positive staining within the inflammatory lesions. No large bacterial colonies were observed. Two of these cases presented clinically with acute septicaemic melioidosis involving the lung and spleen (Case 3 and Case 10 respectively), and the other was a case of asymptomatic latent melioidosis (Case 27) incidentally discovered from a splenectomy specimen following traumatic splenic injury. In acute melioidosis (Case 3, Fig 14, 15 and Case 10, Fig 16,17), the bacilli were visualized both intra- and extracellularly, with the former predominating. The intracellular bacteria occurred either singly or in clusters and were detected predominantly within the cytoplasm of the individual cells that morphologically resemble neutrophils and macrophages, as well as within the 'giant cells' noted in Case 3 (Fig 14: E, F). Some of these intracellular bacteria clusters appeared to have a fairly smooth and rounded border, appearing like 'globi' seen in lepromatous leprosy. Occasional bacterial clusters that appeared to localize within the nucleus of the host cells were also detected (Fig 15: F).

In the case of asymptomatic latent melioidosis involving the spleen (Case 27, Fig 18), a slight difference in bacteria localization is observed. Extracellular clusters of bacilli predominate and they were seen colonizing the necrotic area at the centre of the granulomas. Apart from that, a relatively higher amount of bacteria were detected as compared to the acute melioidosis cases discussed earlier. There were no bacteria detected in non-inflamed tissue or areas remote from the focus of inflammation. No intravascular free-floating bacteria or intracellular bacteria were detected within the circulating phagocytes.

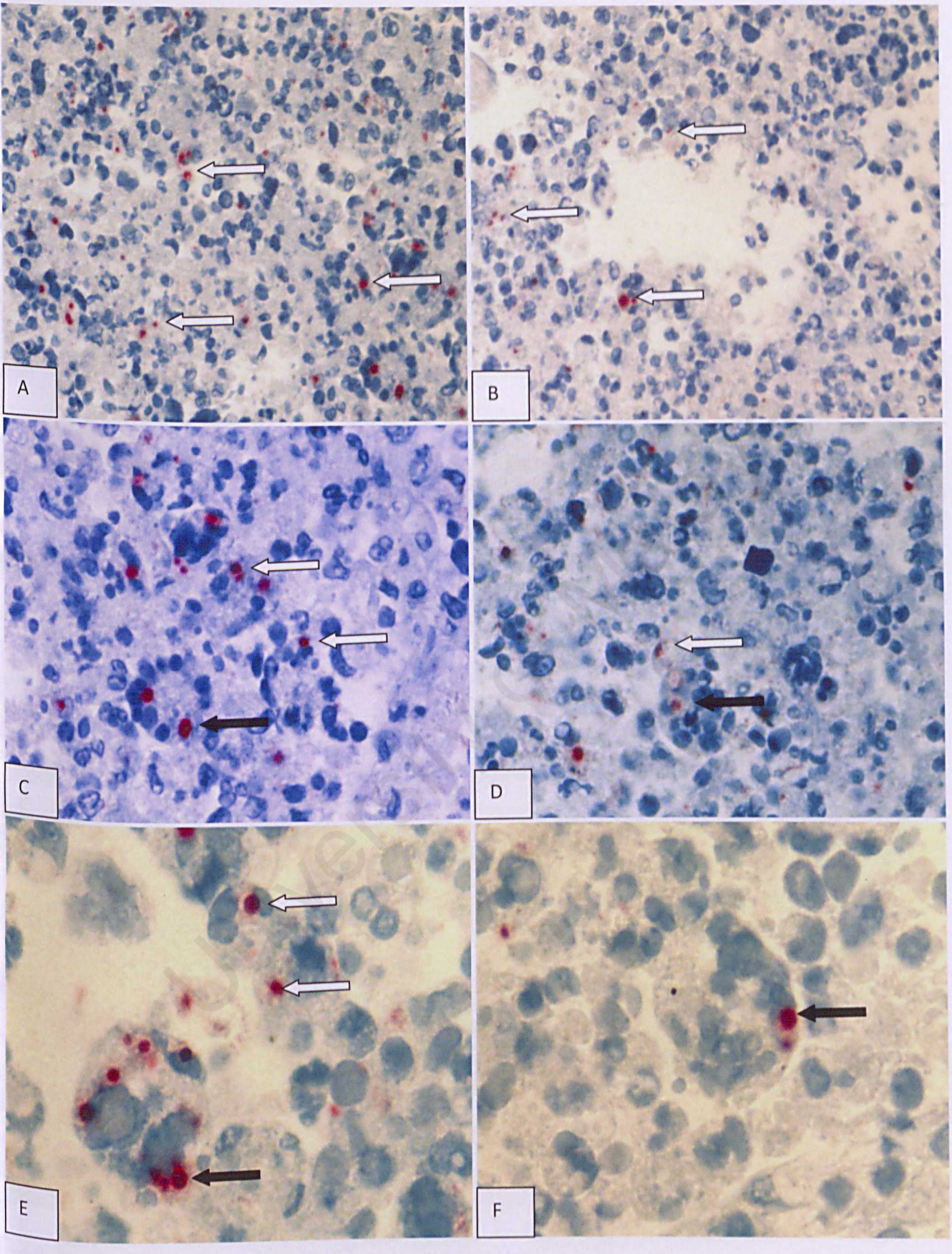

Figure 14: Case 3 [lung]: (A, B) Scattered positive staining (white arrow) were detected at 40x objectives. (C, D, E, F) Higher magnification showing clusters of intracellular bacteria (white arrow), some within 'giant cells' (black arrow).These bacterial clusters had a fairly smooth and rounded border, appearing like 'globi' seen in lepromatous leprosy. (ISH/Liquid permanent red; Magnification: A, B: 40x objective; C, D: 60x objective; E, F: 100x objective)

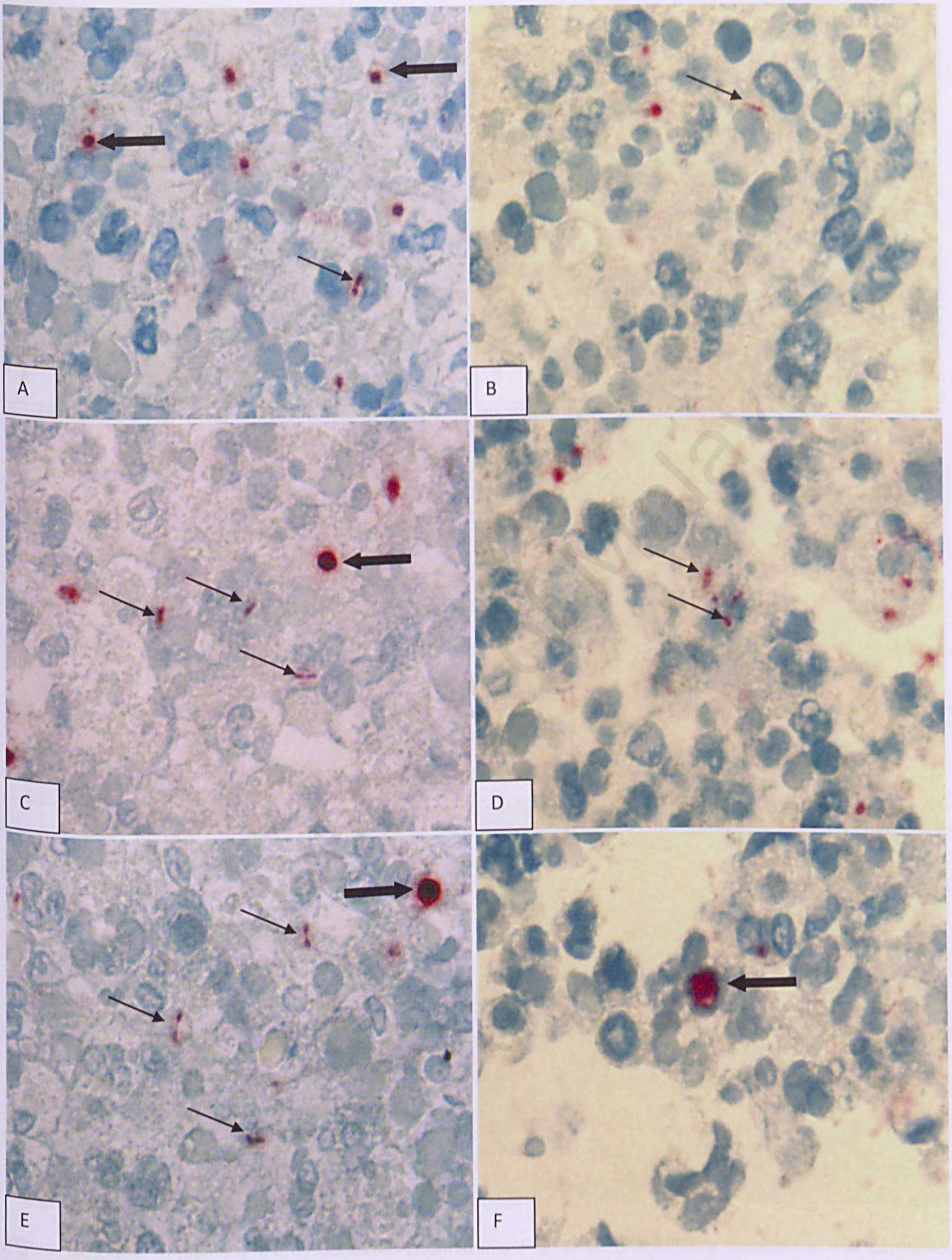

Figure 15: (A, B, C, D, E) Case 3 [lung]: High magnification showing single, isolated rod-shaped bacillus (thin black arrow) and rounded clusters of bacteria (thick black arrow) located within cells morphologically resemble neutrophils and macrophages. (F) Occasional bacterial clusters appeared to be located within the host cell's nuclei. (ISH/Liquid permanent red; Magnification: A, B, C, D, E, F: 100x objective)

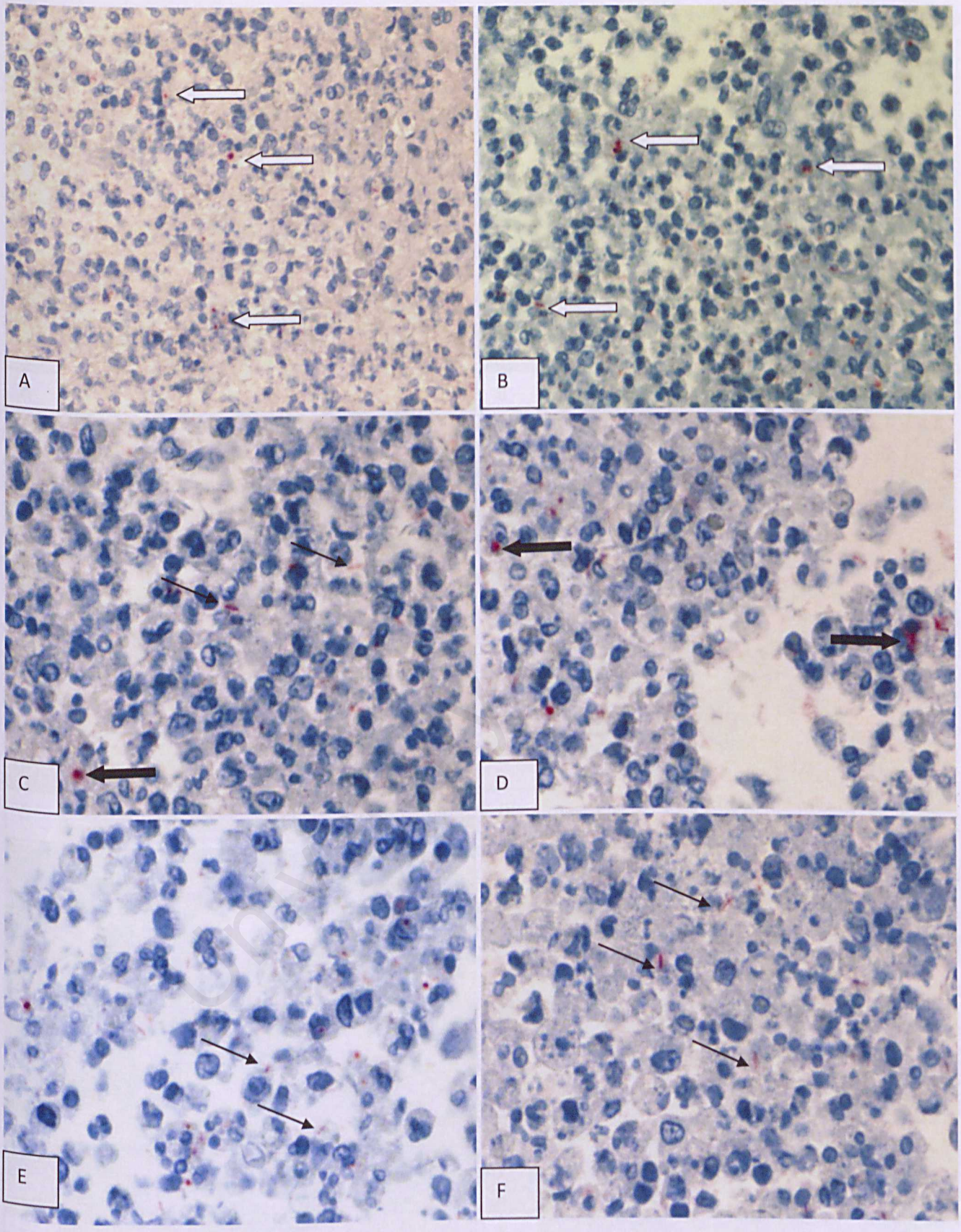

Figure 16: Case 10 [spleen]: (A, B) Scattered positive staining (white arrow) were detected at 40x objective. (C, D, E, F) Single, isolated bacillus (thin black arrow) and rounded clusters of bacteria (thick black arrow) located within inflammatory cells. (ISH/Liquid permanent red; Magnification: A, B: 40x objective; C, D, E, F: 60x objective)

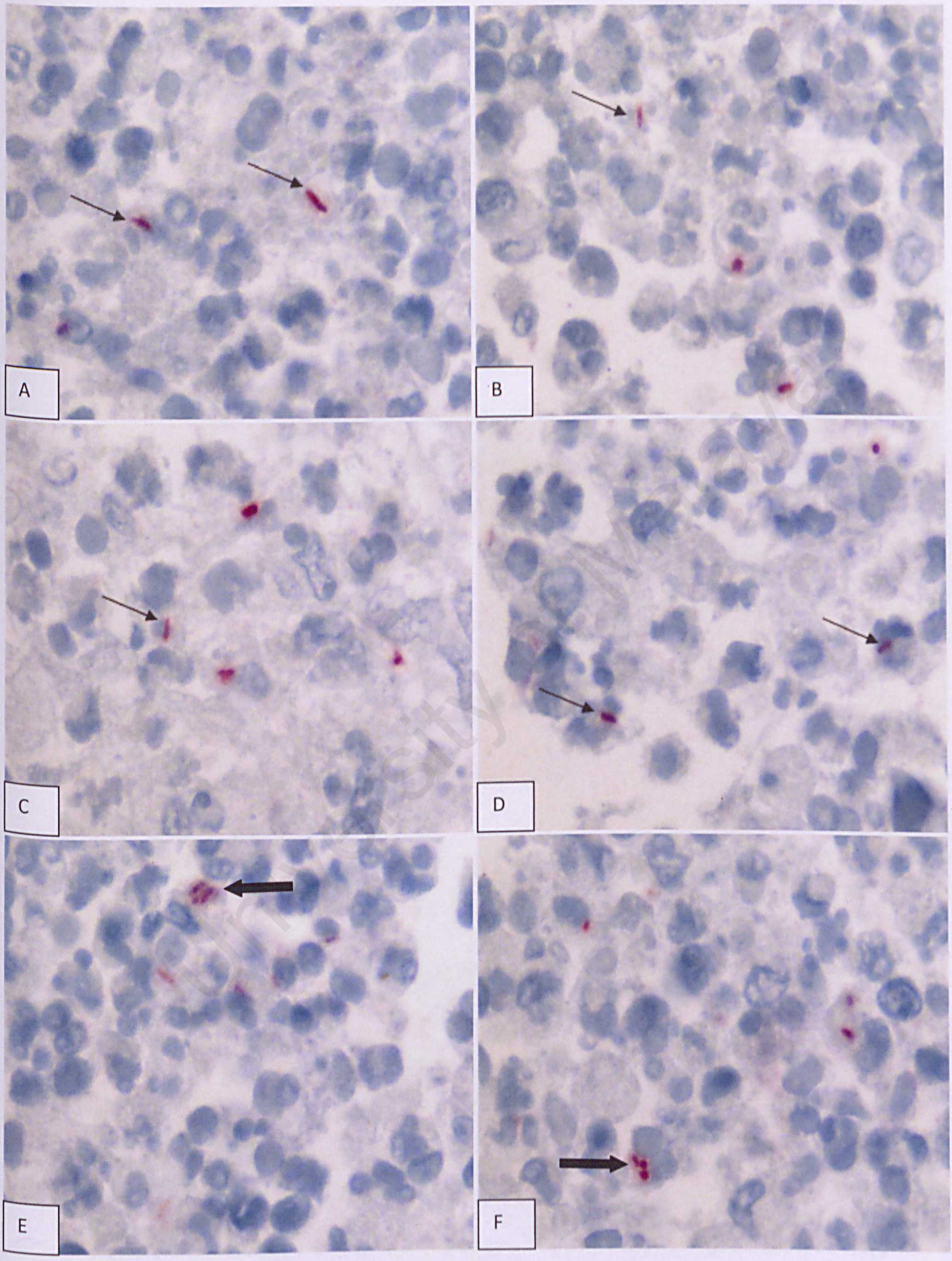

Figure 17: (A, B, C, D, E, F) Case 10 [spleen]: High magnification showing intracellular, single, isolated bacillus (thin black arrow) and clustered bacilli (thick black arrow). (ISH/Liquid permanent red; Magnification: A, B, C, D, E, F: 100x objective)

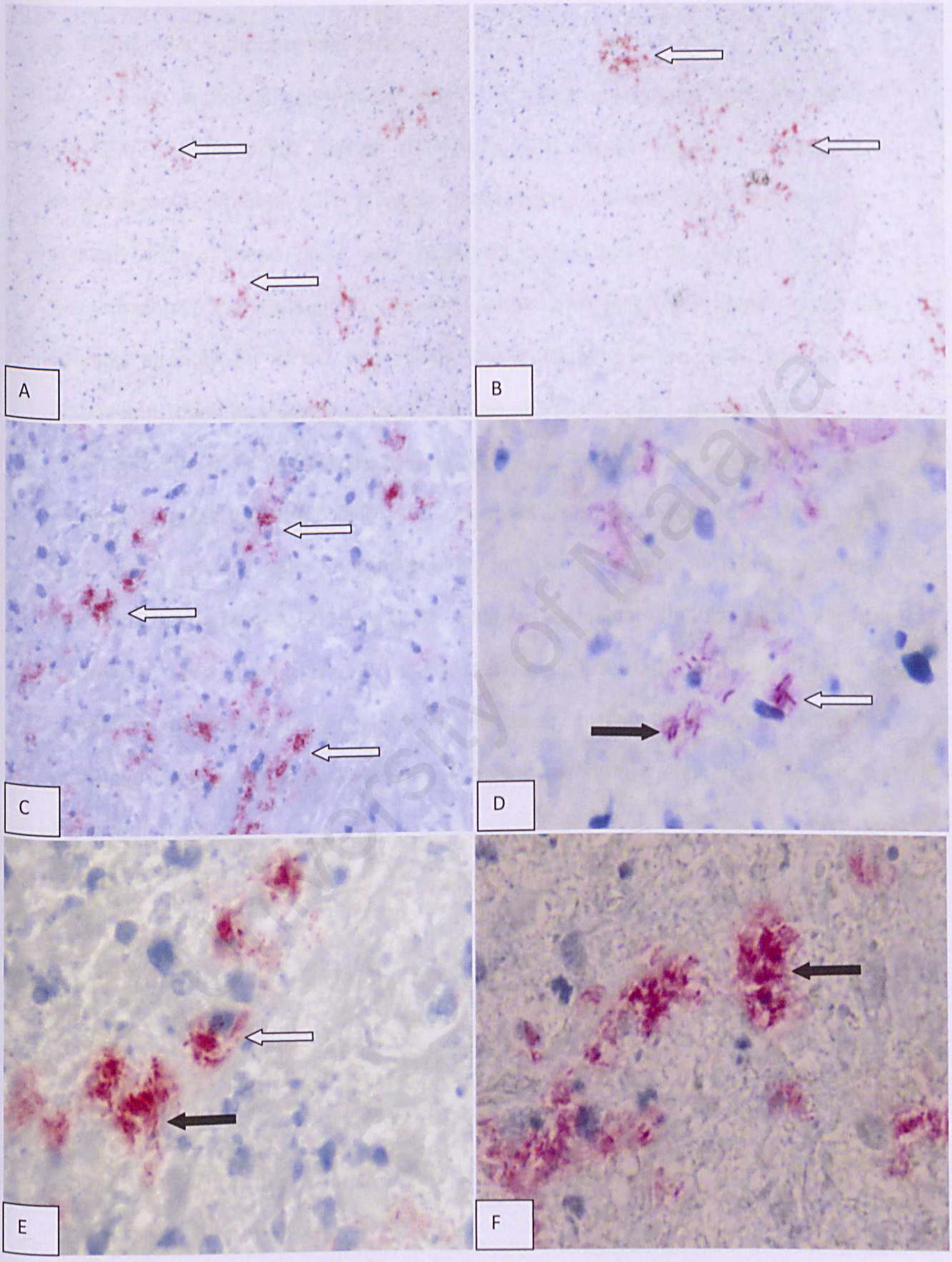

Figure18: Case 27 [spleen]: (A, B, C) Scattered positive staining (white arrow) were detected in the necrotic areas within the granulomas. (D, E, F) Higher magnification showing large clusters of extracellular bacilli (black arrow) and a few clusters of possibly intracellular bacilli (white arrow). (ISH/Liquid permanent red; Magnification: A, B: 10x objective; C: 40x objective; D, E, F: 100x objective)

4. 'Giant cells' in acute melioidosis

Four immunohistochemical stains, a broad spectrum epithelial marker (CKAE1/3), a histiocytic marker (CD68), a granulocytic marker (CD15) and a megakaryocytic marker (CD61) were performed in an attempt to determine the cellular origin of these 'giant cells' observed in lung tissue in Case 3 (Fig 3, 4). Unsurprisingly, the majority of the cells within the abscesses were neutrophils staining strongly for CD15 and focally these CD15 positive cells appeared to fuse/clump together leading to the formation of the so called 'giant cells' (Fig 19). CD68 (Fig 20: A), CD61 (Fig 20: B) and CKAE1/AE3 (Fig 21) were negative. These findings suggest that the 'giant cells' observed in acute severe melioidosis were likely due to cellular fusion, and particularly in this case, fusion of neutrophils. Apart from that, the negative CD61 and CD68 expressions indicate that the 'giant cells' are unlikely to be megakaryocytes or classical multinucleated giant cells (such as Langhan's and foreign body type) that are typically histiocytic in origin. Neither are the fused cells epithelial cells such as pneumocytes/surface epithelial cells that line the alveolar spaces.

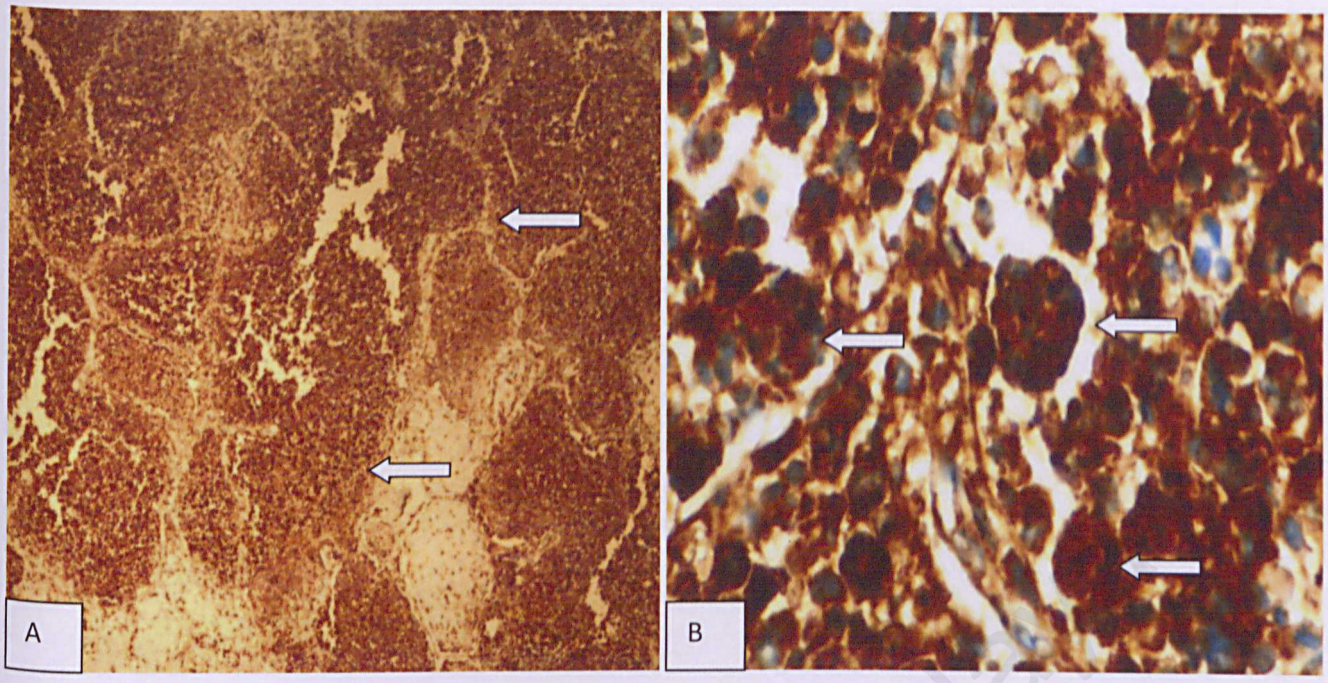

Figure 19: Case 3 [lung, CD15] (A) Low magnification showing diffuse sheets and dense aggregates of CD15 positive neutrophils within the alveolar spaces forming abscesses (arrow). (B) High magnification showing CD15 positive neutrophils that appeared to fuse/clump together forming the so called 'giant cells' (arrow). (Immunoperoxidase; Magnification: A: 4x objective; B: 60x objective)

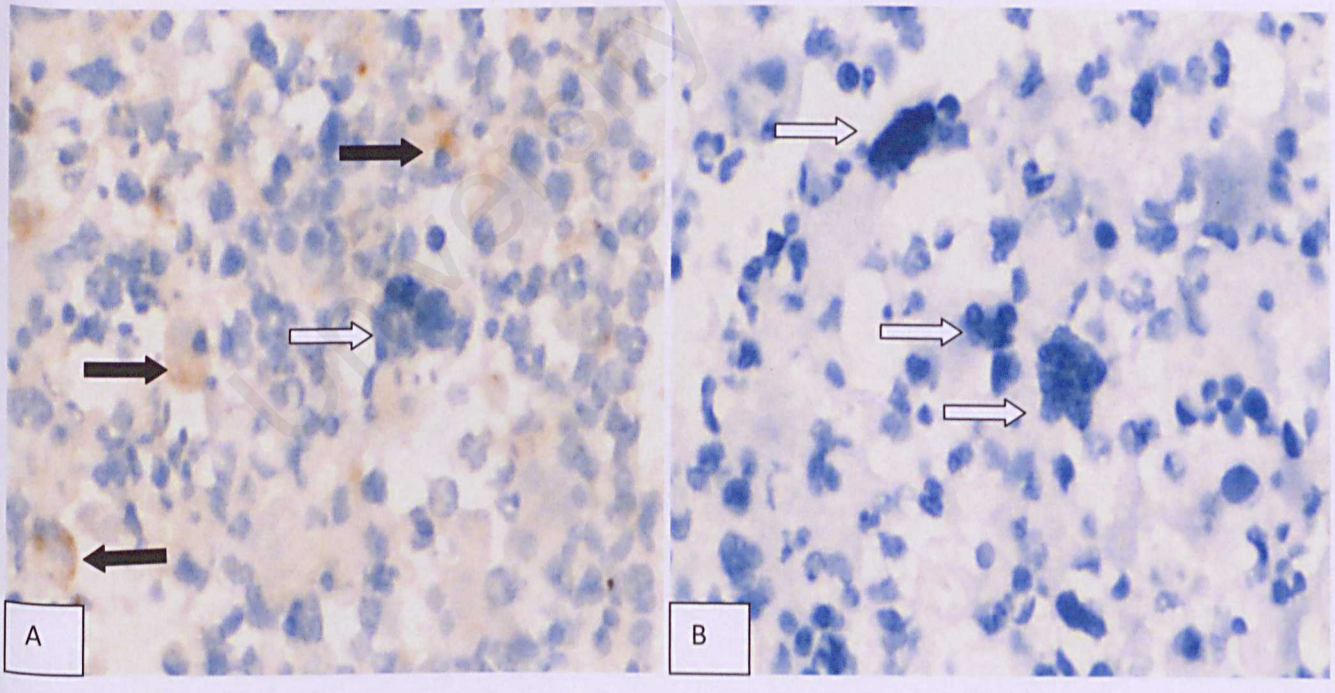

Figure 20: (A) Case 3 [lung, CD68]: Scattered alveolar macrophages (black arrow) were highlighted by CD68. 'Giant cells' (white arrow) were negative. (B) Case 3 [lung, CD61]: 'Giant cells' (white arrow) were also negative for CD61. (Immunoperoxidase; Magnification: A, B: 60x objective)

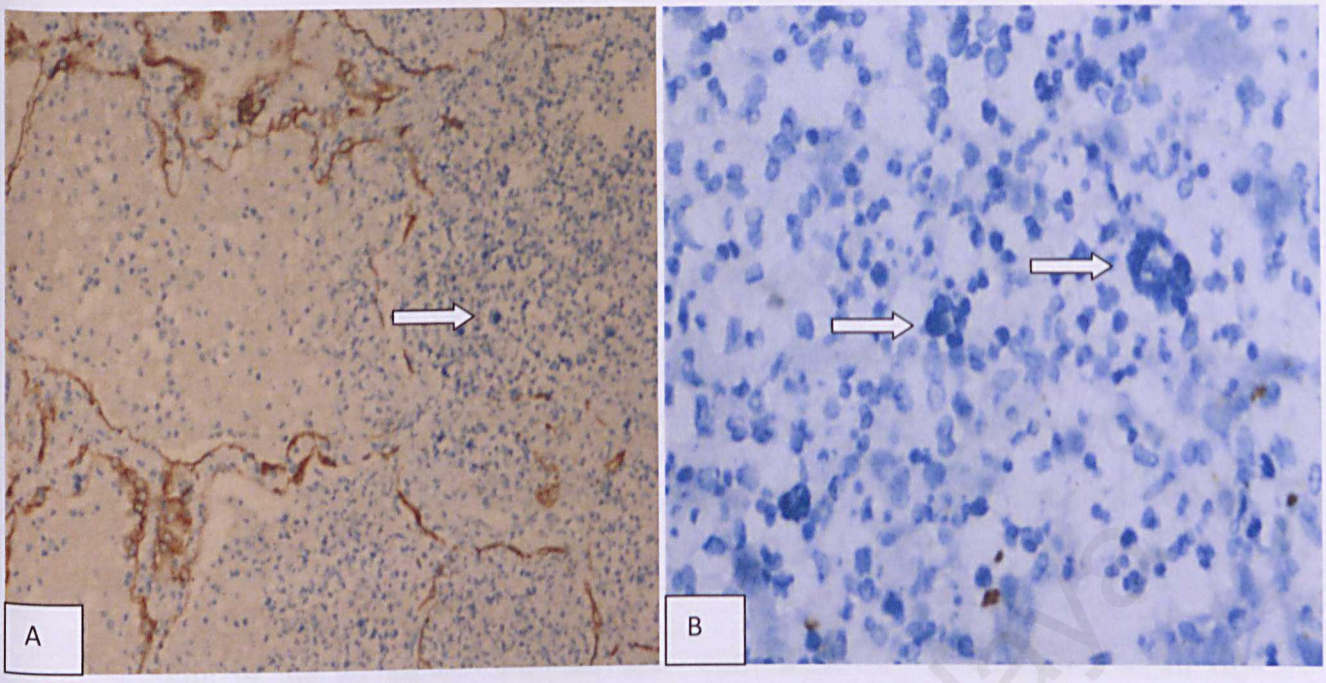

Figure 21: Case 3 [lung, CKAE1/3]: (A, B) 'Giant cells' (arrow) were negative for CKAE1/3. The intact surface epithelial cells lining the alveolar spaces/pneumocytes served as internal positive control. (Immunoperoxidase; Magnification: A: 10x objective; B: 40x objective)

DISCUSSION

Melioidosis is not commonly encountered in diagnostic surgical pathology as antimicrobial therapy is still the mainstay of treatment. This is reflected by our study where from a total of 619 *Burkholderia pseudomallei* isolates from the microbiology laboratory of Hospital Pulau Pinang (HPP) (2003-2016) and Hospital Raja Permaisuri Bainun Ipoh (HRPBI) (2010-2015), 238 culture positive cases were identified and from these only 27 cases required surgical intervention for various reasons.

Out of the 27 cases, infected skin, soft tissue (7), and osteo-articular (6) tissues together constituted almost half of the surgical pathology specimens studied. These are probably the most common specimens encountered in histopathology laboratories, as they are often more superficial, easily accessible and operable. These cases were then followed by lung/pleura (4), spleen (4) and liver (1). As in most series, pneumonia or pleural effusion was reported as the most common presentation of melioidosis[27]. Therefore specimens from these sites were expected to be seen quite frequently in a surgical pathology laboratory. Besides that, abscesses in the internal organs such as the liver and spleen were also common presentations. Liver involvement was identified in up to 4 cases in this study, but only one resection specimen was submitted for histopathological examination. A case of genitourinary infection involving the testis was also included. However, prostatic infection which was reported to be fairly common in Australia and requiring drainage was not encountered in this study [30, 31]. Focal suppurative infections involving the central nervous system were not uncommon[27]. Some of these may represent direct spread from contiguous sites, such as facial sinuses or orbital cellulitis. Primary meningitis has also been observed in Thailand[28] but more often results from ruptured

cerebral abscesses[29]. In this study, a case of brain abscess involving the meninges (dura) was seen whereby the patient presented with headache and focal neurological deficit. Melioidosis involving the ENT/head and neck region which was claimed to be relatively uncommon[25], were encountered in two cases. The first case is a 6 years old child with no known risk factors, who presented with parapharyngeal abscess and cervical necrotizing suppurative lymphadenitis (Case 8). The second case is a case of parotid abscess seen in a patient with multifocal melioidosis involving both spleen and liver. The parotid abscess was drained by fine needle aspiration and the pus was sent for cytology assessment. The cytology smear showed abundant neutrophils consistent with acute suppurative inflammation. However the cell block preparation was considered unsatisfactory due to scant cellularity.

The main predisposing factor identified in this study is still diabetes mellitus. This is comparable to the latest (2016) local review conducted in Hospital Universiti Sains Malaysia (HUSM), Kubang Kerian, Kelantan, Malaysia, but lower in rate (40.7%, n=27) as compared to the HUSM cases (74.7%, n= 133) [26]. This could be partly due to incomplete clinical information provided by clinicians in the histopathological request forms. Other predisposing factors identified include renal transplant, malignancy (e.g. lymphoma), parenteral drug abuse and chronic lung diseases such as pulmonary tuberculosis and bronchial asthma. Bacteraemia was reported in majority of the HUSM cases (76.6%, n=121). It was seen in more than half of the cases in this study (55.6%, n=27).

Accurate diagnosis of melioidosis cannot be made in most of the cases based on histopathological findings alone. This is still very true as both the acute and chronic inflammations observed in this study were non-specific. For example, chronic

pulmonary melioidosis presented with upper lobe consolidation and cavitation (as in Case 15, Fig 11: E) had been reported to be closely mimicking tuberculosis histologically, as well as clinically and radiographically[23]. As another illustration of this fact, necrotizing lymphadenitis caused by *B. pseudomallei* infection (as in Case 8, Fig 8: A, B) could potentially lead to wrong diagnosis of cat scratch disease in the absence of microbiological correlation[24]. However, the presence of cell-to-cell fusion leading to 'giant cell' formation in a background of acute necrotizing inflammation appeared to be a helpful diagnostic clue to severe acute melioidosis. The histopathologist may alert the clinician so that the appropriate microbiological work-up is being carried out. It is important to note that high index of suspicion should always be practiced in endemic areas like Malaysia, especially in the presence of risk factors such as diabetes mellitus, chronic renal failure, excessive alcohol intake, steroid intake or history of exposure. In addition, with the availability of ancillary test such as ISH, the diagnostic process may be sped up, as compared to traditional bacterial culture that may take several days to be completed. This could be potentially lifesaving in an acutely ill patient.

The sensitivity of *in situ* hybridization (ISH) assay in detecting *B. pseudomallei* appears to be poor in this study. Out of the total 27 cases, only 3 cases showed positive *in situ* hybridization results. This was presumably due to the low bacterial load in surgical pathology specimens as most of the patients were subjected to antimicrobial therapy prior to surgical interventions. Furthermore, it is likely that when the surgeries were performed, patients were already stable clinically and recovering from the infection. The sensitivity of the assay was also largely dependent on the quality of the specimens and the amount of tissue available for testing: small biopsies submitted by clinician may not be representative of the whole lesion, and in

this study, 20 out of the 27 cases were biopsies. As for fine needle aspiration cytology specimens and cell block preparations, the cellularity of the specimen and the technique of the aspirator are of great importance. There is always a possibility that the lesional tissue/cells were missed if the procedures were done blindly without imaging guidance. Moreover, the inconsistent results due to variations in tissue fixation, processing, optimal pretreatment and digestion steps in ISH from sample to sample cannot be overemphasized. Finally, bone biopsies undergoing decalcification process may suffer significant DNA and RNA degradation leading to potential false negative results, as most of the surgical pathology laboratories in Malaysia are using strong (hydrochloric acid, nitric acid) or weak acids (formic acid) decalcifiers for routine surgical pathology specimens. Chelating agents such as ethylenediaminetetracetic acid (EDTA) that slowly work by capturing the calcium ions are considered to be more suitable for molecular techniques such as ISH or PCR[37].

The specificity of the ISH assay was otherwise believed to be good. The probe specificity was confirmed by Eu et al[13] during the initial probe development via Basic Local Alignment Search Tool (BLAST) sequence analysis and by testing on appropriate microbial controls, which includes *B. cepacia*, *B. thailandensis* and 16 non-*Burkholderia* microorganisms (Appendix 2). The probe did not hybridize with the non-*Burkholderia* microorganisms and *B. cepacia*. However, cross-hybridization with *B. thailandensis*was observed. This was most likely because *B. pseudomallei* and *B. thailandensis* shared >90% homology in the targeted rRNA region[13]. Fortunately, *B. thailandensis* is an avirulent, non-pathogenic *Burkholderia* species[35,36] that is less likely to be encountered in surgical pathology specimens. Another organism that was predicted to show cross-hybridization (100% nucleotide homology) but not being tested was *B. mallei*[13]. Fortunately, both *B. thailandensis* and *B. mallei* infections are

rare compared with *B.pseudomallei* in endemic areas and less likely to be encountered in clinical materials/tissue specimens. In this study, additional negative controls consisted of human tissues known to be infected by several fungal organisms and other bacteria were included and they were all tested negative.

All the three cases that showed positive ISH results were large organ resection specimens, where multiple tissue blocks were available for ISH testing. In acute melioidosis (Case 3, Fig 14, 15 and Case 10, Fig 16, 17), the positively-stained bacteria were found mostly intracellularly. This is consistent with the well-established fact that *B. pseudomallei* are capable of intracellular survival and multiplication. The cellular pathogenesis of *B. pseudomallei* infection involves attachment, entry, and internalization within membrane bound vacuoles, which progressively acidifies and develops into a mature degradative phagolysosome[21]. It was reported that *B. pseudomallei* can survive the phagolysosome either by preventing vacuole-lysosome fusion or by modifying the acidic environment within the phagolysosome. Moreover, the bacterium has also evolved to escape from the vacuole and survive within the cytosol[22]. This confirmed that the well-stained single isolated bacilli and clusters of bacteria with rounded configurations seen in the cytoplasm highlighted by ISH were true and not merely artifacts. The overall morphological appearance of intact bacilli suggests that the bacteria are viable.

In chronic latent melioidosis (Case 27, Fig 18), a relatively larger amount of bacteria were detected. This could possibly be explained by the fact that the patient was asymptomatic and no antimicrobial therapy was administered prior to the surgery. It is worth mentioning here that ISH testing was particularly useful in diagnosing *B. pseudomallei* infection in this case as melioidosis was not suspected initially and no fresh tissue/specimen was sent for culture studies. The patient was

diabetic and presented with traumatic splenic injury following motor vehicle accidents. His splenectomy specimen was incidentally found to have granulomas that were subsequently proven to be *B. pseudomallei* infected with ISH and further confirmed by DNA sequencing. He developed surgical wound infection at Day 4 post-op and multiple superficial abscesses around abdominal scar 16 months later. Cultures taken from these sites at later dates were both positive for *B. pseudomallei*.

Recently, intranuclear localization of *B. pseudomallei* was also being demonstrated by Vadivelu et al[17] via transmission electron microscopy (TEM) in human autopsy tissue. The occurrence of bacteria clusters within the nucleus of infected cells with ISH (Fig 16, F) further supports this observation. It was postulated that the nucleus may have played a role as an occult or transient niche for persistence of intracellular pathogens in a latency state, and potentially leading to recurrent episodes or recrudescence of *B. pseudomallei* infection, which is a striking characteristic of this infection[17].

In conclusion, ISH appeared to have a useful role in the diagnosis of melioidosis, though the sensitivity is not as good as bacterial culture. The specificity was believed to be good. However further testing with other molecular techniques such as PCR and DNA sequencing need to be performed to confirm this and larger study ideally has to be carried out to validate our findings. ISH has an advantage in that it is applicable to a variety of specimen types, including fresh or frozen tissue, cytologic preparations, and formalin-embedded tissue though the sensitivity varies. It had also been suggested that this method could be applied directly on smears for bacterial identification using bodily fluids or pus[13]. Further tests should be performed to evaluate the usefulness of this assay for various clinical diagnostic purposes.

REFERENCES

1. Abu Bakar AN, Amirullah MA, How SH et al. Guideline for clinical and public health management of melioidosis in Pahang. Ministry of Health, Malaysia.
2. Puthucheary SD, Vadivelu J. Human Melioidosis. Singapore University Press 2002
3. How SH, Ng KH, Jamalludin AR, Shah A, Rathor Y. Melioidosis in Pahang. Malaysia Med J 2005; 60(5):606-613
4. Puthucheary SD. Melioidosis in Malaysia. Med J Malaysia 2009;64:266–274
5. Strauss JM, Alexander AD, Rapmund G, Gan E, Dorsey AE.Melioidosis in Malaysia III: Antibodies to *Pseudomonas pseudomallei* in the human population. Am J Trop Med Hyg 1969; 1:703-707
6. Puthucheary SD. The laboratory diagnosis of meliodosis. Selected papers from the 1st International Symposium on Melioidosis, Kuala Lumpur, April, 7-8, 1994. SP-Muda Printing Sdn. Bhd Kuala Lumpur
7. Wong KT, Puthucheary SD, Vadivelu J. The histopathology of human melioidosis. Histopathology1995; 26:51–55.
8. Wong KT, Vadivelu J, Puthucheary SD, Tan KL. An immunohistochemical method for the diagnosis of melioidosis. Pathology 1996; 28:188-191.
9. Ho CC, Lau CC, Martelli P et al. A novel pan-genomic analysis approach in target selection for multiplex PCR identification and detection of *Burkholderiapseudomallei*, *Burkholderiathailandensis* and *Burkholderiacepac ia* complex species: a proof-of-concept study. J ClinMicrobiol 2011; 49:814–821.

10. Meumann EM, Novak RT, Gal D et al. Clinical evaluation of a type III secretion system real-time PCR assay for diagnosing melioidosis. J ClinMicrobiol 2006; 44:3028–3030.

11. Hagen RM, Gauthier YP, Sprague LD et al. Strategies for PCR based detection of *Burkholderia pseudomallei* DNA in paraffin wax embedded tissues. MolPathol 2002; 55:398–400.

12. Schmoocl G, Ehricht R, Melzer F *et al.* DNA microarray-based detection and identification of *Burkholderia mallei*, *Burkholderia pseudomallei* and *Burkholderia spp*. Mol Cell Probes 2009;23:178–187.

13. Eu LC, Ong KC, Hiu J, Vadivelu J, Nathan S, Wong KT, 2014. In situ hybridization to detect and identify *Burkholderia pseudomallei* in human melioidosis. Mod Pathol 27: 657-664.

14. Hagen RM, Frickmann H, Elschner M et al. Rapid identification of *Burkholderia pseudomallei* and *Burkholderia mallei* by fluorescence *In situ* hybridization (FISH) from culture and paraffin-embedded tissue samples. Int J Med Microbiol 2011; 301:585–590.

15. Chow TK, Eu LC, Chin KF et al. Incidental Splenic Granuloma Due to *Burkholderia pseudomallei*: A Case of Asymptomatic Latent Melioidosis? Am J Trop Med Hyg 2016; 94(3):522-524

16. Pruksachartvuthi S, Aswapokee N, Thankerngpol K. Survival of *Pseudomonas pseudomallei* in human phagocytes. J Med Microbiol 1990; 31: 109-114.

17. Vadivelu J, Vellasamy KM, Thimma J et al. Survival and Intra-Nuclear Trafficking of Burkholderia pseudomallei: Strategies of Evasion from Immune

Surveillance? PLoSNegl Trop Dis 2017; 11 (1): e0005241. doi:10.1371/journal.pntd.0005241

18. Kespichayawattana W, Rattanachetkul S, Wanun T, Utaisincharoen P, Sirisinha S.*Burkholderia pseudomallei* induces cell fusion and actin-associated membrane protrusion: a possible mechanism for cell-to-cell spreading. Infect Immun 2000; 68: 5377–5384.
19. Welkos SL, Klimko CP, Kern SJ et al. Characterization of *Burkholderia pseudomallei* Strains Using a Murine Intraperitoneal Infection Model and In Vitro Macrophage Assays. PLoS ONE 2015; 10(4): e0124667. doi:10.1371/journal.pone.0124667
20. Greenawald KA, Nash G, Foley FD. Acute systemic melioidosis. Am J ClinPathol 1969; 52:188–198.
21. Tandhavanant S, Thanwisai A, Limmathurotsakul D, et al. Effect of colony morphology variation of *Burkholderia pseudomallei*on intracellular survival and resistance to antimicrobial environments in human macrophages in vitro.BMCMicrobiol2010; 10:303.
22. Stevens MP, Wood MW, Taylor LA, et al. An Inv/Mxi-Spa-like type III protein secretion system in *Burkholderia pseudomallei* modulates intracellular behavior of the pathogen. MolMicrobiol2002; 46:649-659
23. Spotnitz M, Rudnitzky JR, Rambaud JJ.Melioidosis pneumonitis. JAMA 1967; 202: 950-954.
24. Yee KC, Lee MK, Chua CT, Puthucheary SD. Melioidosis, the great mimicker: a report of 10 cases from Malaysia. J Trop Med Hyg 1988; 92:249-254.
25. Lim WK, Gurdeep GS, Norain K.Melioidosis of the Head and Neck. Med J Malaysia 2001;56(4):471-477

26. Zueter AR, Abumarzouq M, Rahman ZA, Deris ZZ, Harun A. The epidemiology and clinical spectrum of melioidosis in a teaching hospital in a North-Easthern state of Malaysia: a fifteen-year review. BMC infectious diseases.2016; 16(1):333.

27. Cheng AC, Currie BJ. Melioidosis: epidemiology, pathophysiology, and management. Clin Microbiol Rev. 2005;18(2):383-416

28. Saipan, P. Neurological manifestations of melioidosis in children. Southeast Asian J. Trop. Med. Public Health. 1998; 29:856-859

29. White, N.J. Melioidosis. Lancet. 2003; 361:1715-1722.

30. Currie B, Howard D, Nguyen VT, Withnall K, Merianos A. The 1990-1991 outbreak of melioidosis in the Northern Territory of Australia: clinical aspects. Southeast Asian J. Trop. Med. Public Health 1993; 24:436-443

31. Currie BJ, Fisher DA, Howard DM et al. Endemic melioidosis in tropical northern Australia: a 10-year prospective study and review of the literature. Clin. Infect. Dis. 2000; 31: 981-986

32. Bashir DM. *In situ* hybridization for the identification of *Helicobacter pylori* in paraffin wax embedded tissue. J ClinPathol 1994; 47:862–864.

33. Hogardt M, Trebesius K, Geiger AM et al. Specific and rapid detection by fluorescent *In situ* hybridization of bacteria in clinical samples obtained from cystic fibrosis patients. J ClinMicrobiol 2000; 38:818–825.

34. Palasubramaniam S, Muniandy S, Navaratnam P. Rapid detection of ESBL-producing *Klebseilla pneumoniae* in blood cultures by fluorescent in-situ hybridization. J Microbiol Methods 2008; 72:107–109.

35. Brett PJ, DeShazer D, Woods DE. *Burkholderia thailandensis* sp. nov., a *Burkholderia pseudomallei*-like species. Int J SystBacteriol 1998; 48:317–320.

36. Smith MD, Angus BJ, Wuthiekanun V et al. Arabinose assimilation defines a nonvirulent biotype of *Burkholderia pseudomallei*. Infect Immun 1997; 65:4319–4321.

37. Singh VM, Salunga RC, Huang VJ et al. Analysis of the effect of various decalcification agents on the quantity and quality of nucleic acid (DNA and RNA) recovered from bone biopsies. Ann Diagn Pathol. 2013 Aug; 17(4):322-326

APPENDIX 1

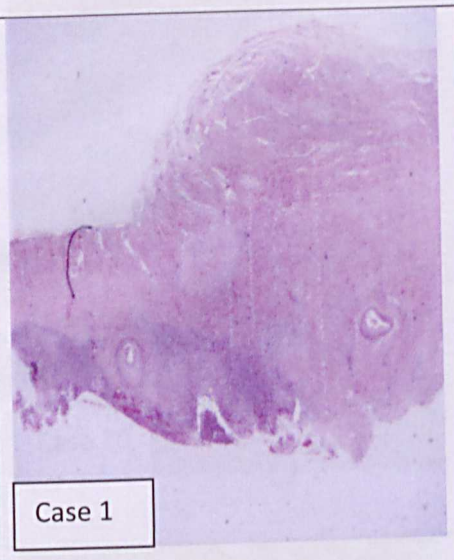
Case 1

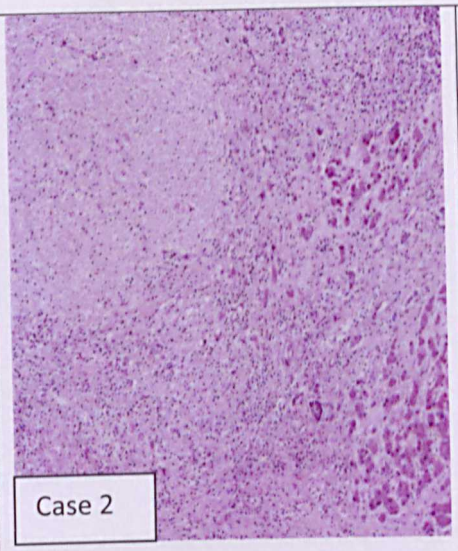
Case 2

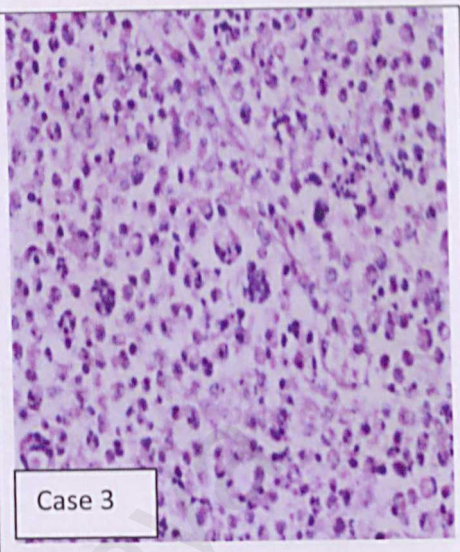
Case 3

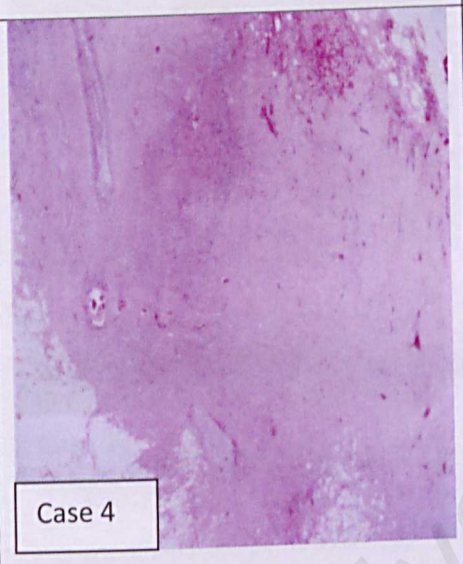
Case 4

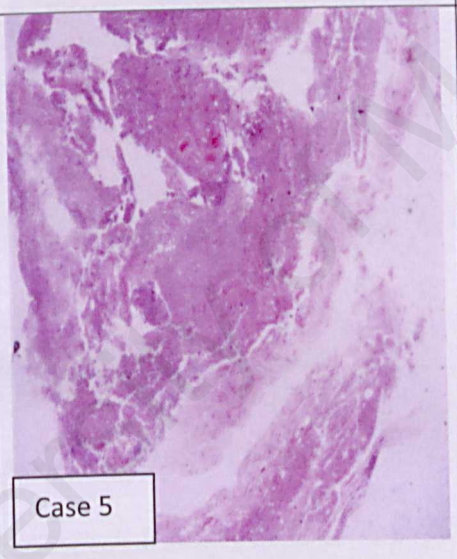
Case 5

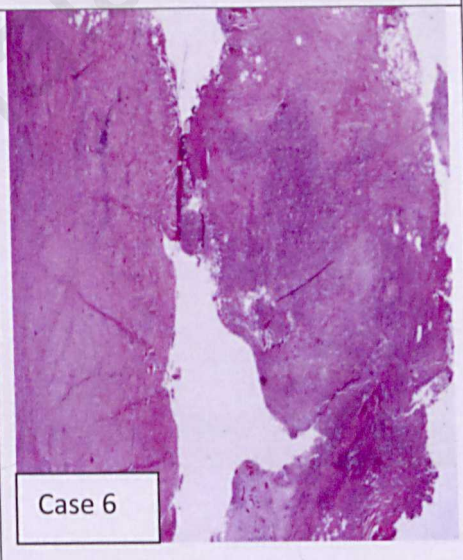
Case 6

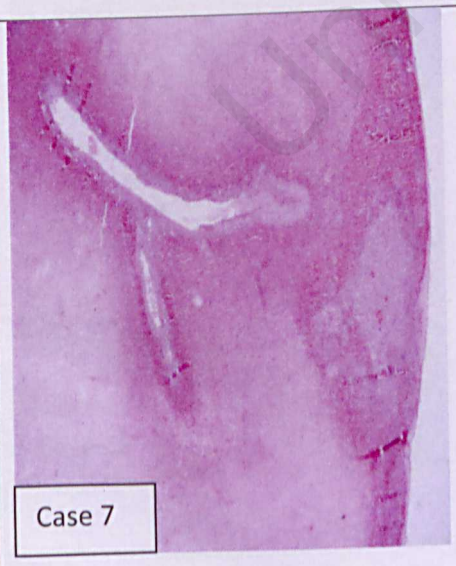
Case 7

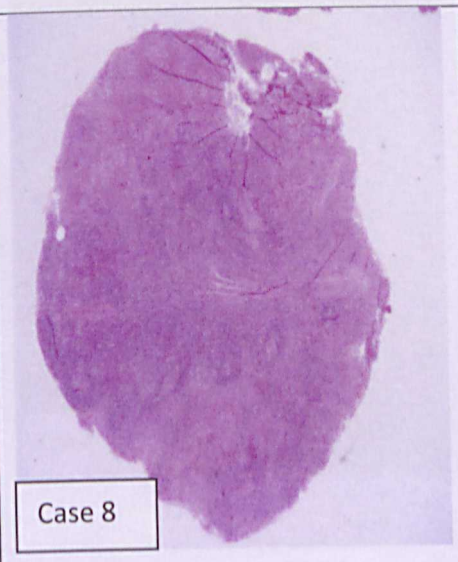
Case 8

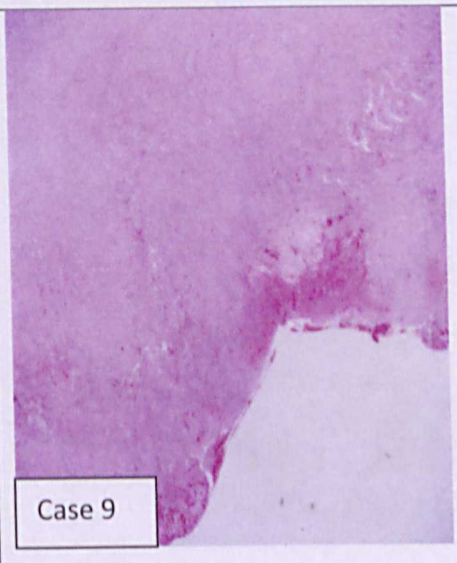
Case 9

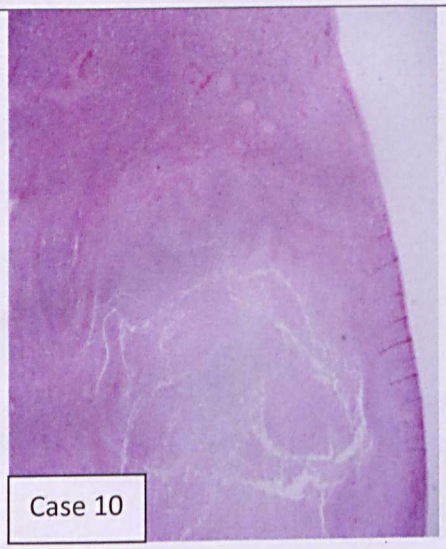
Case 10

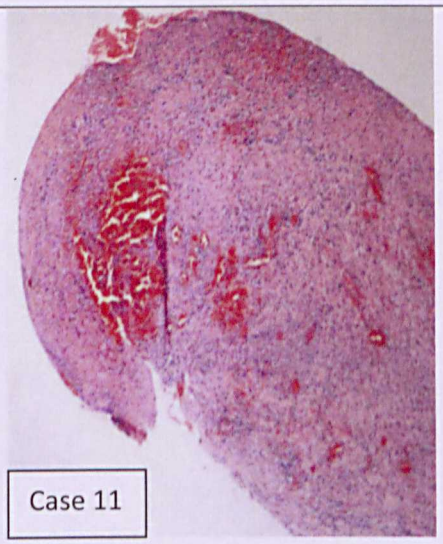
Case 11

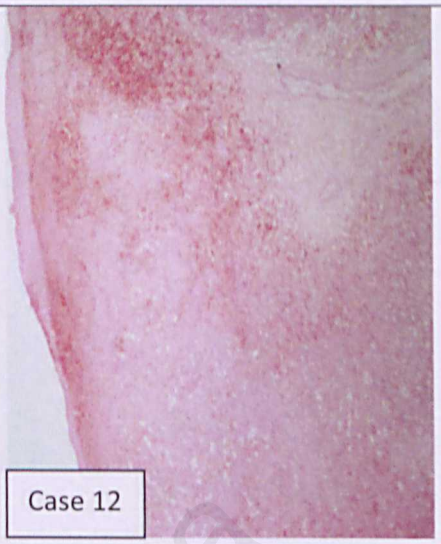
Case 12

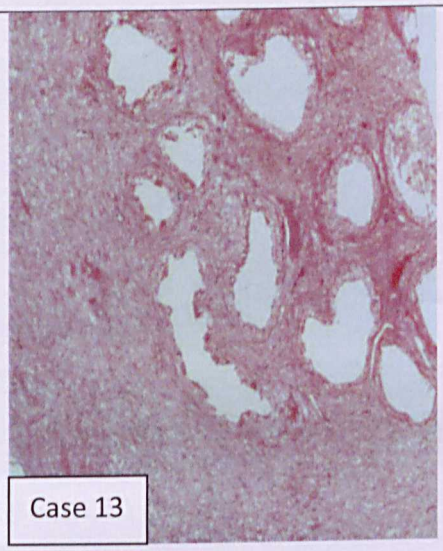
Case 13

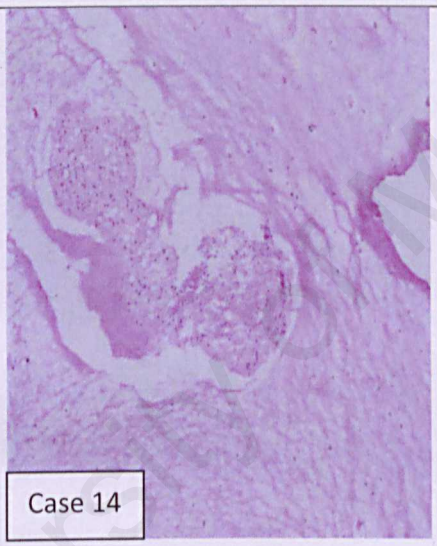
Case 14

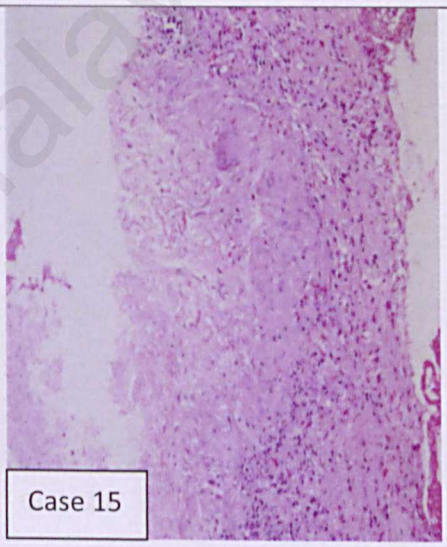
Case 15

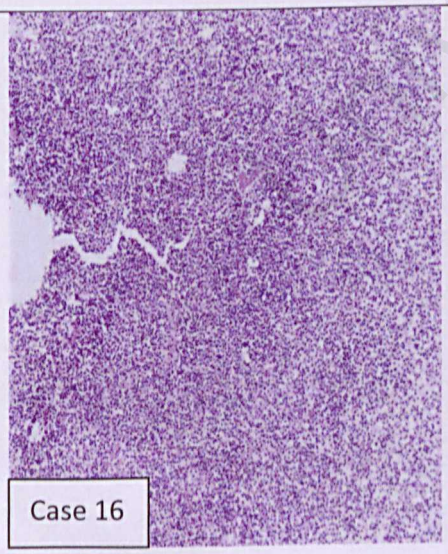
Case 16

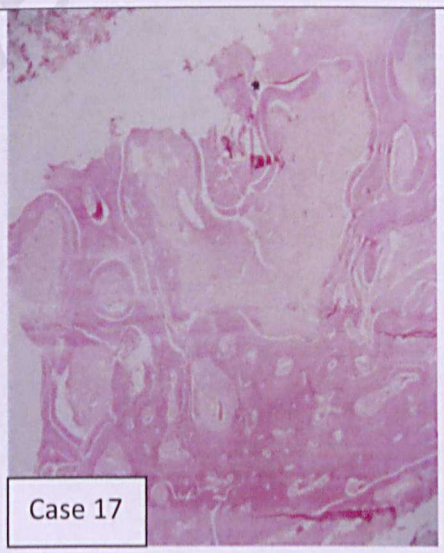
Case 17

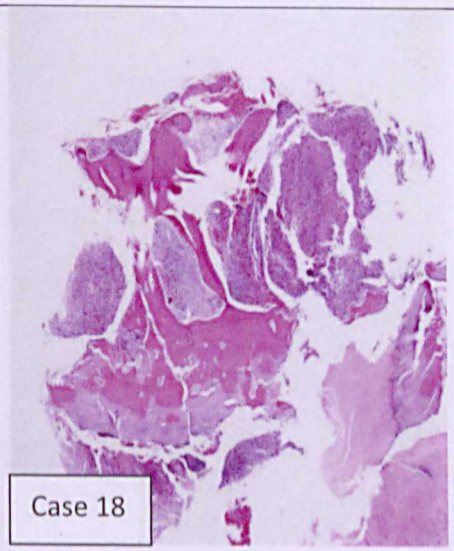
Case 18

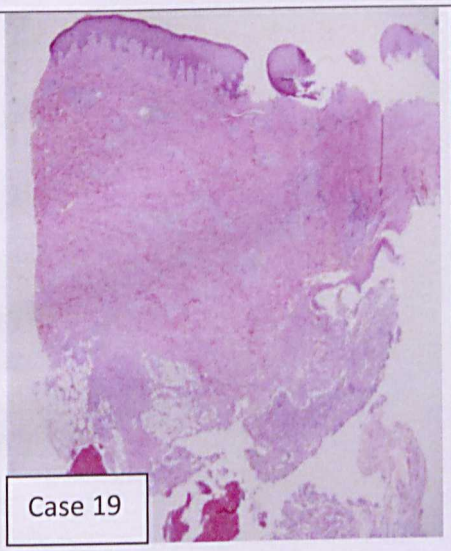
Case 19

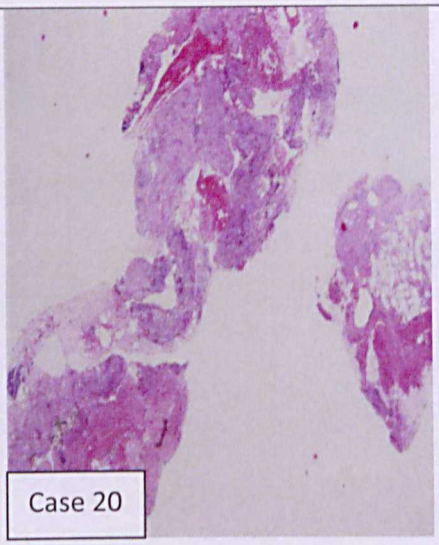
Case 20

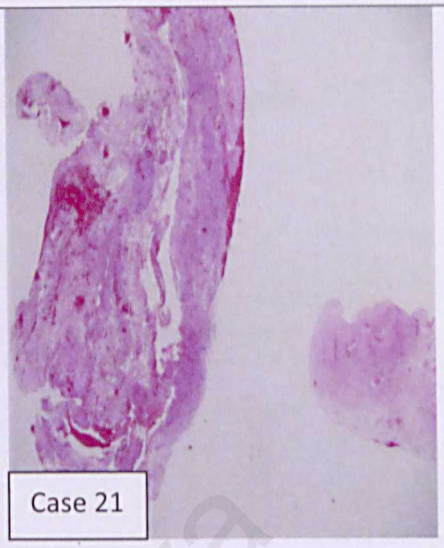
Case 21

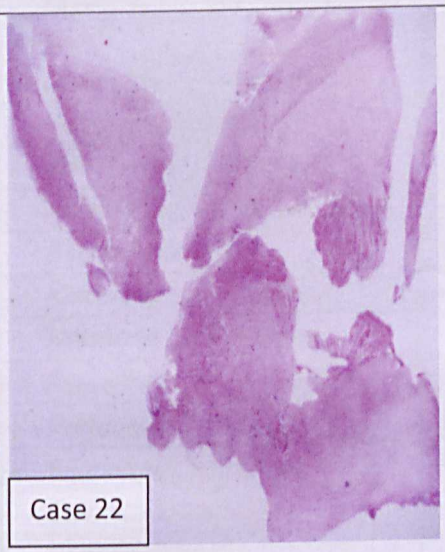
Case 22

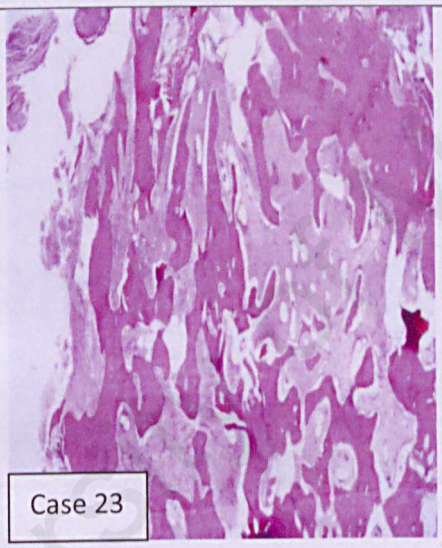
Case 23

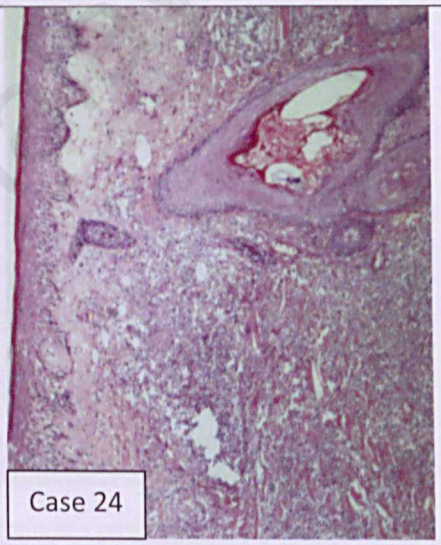
Case 24

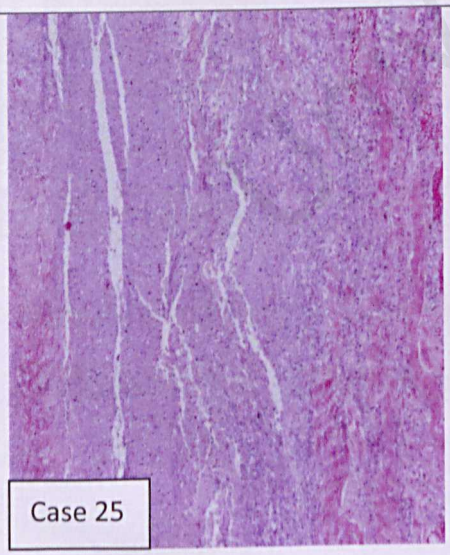
Case 25

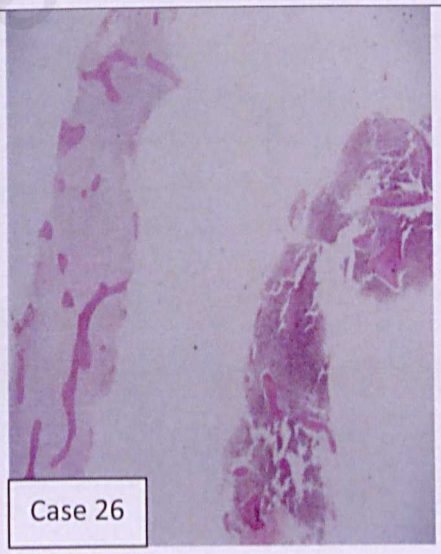
Case 26

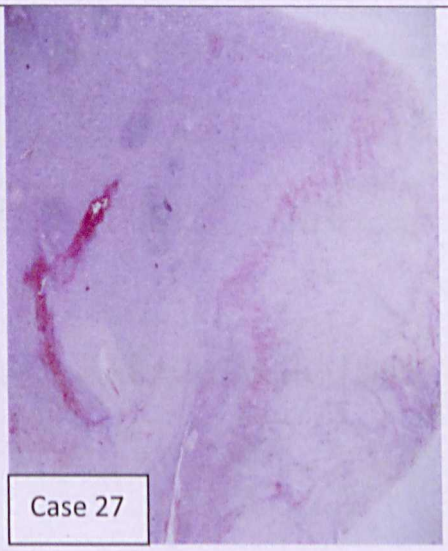
Case 27

APPENDIX 2

Results of *in situ* hybridization specificity testing performed on control microorganisms (adapted from Eu et al[13])

	Results	
Microorganisms	***Microorganism cell smears on glass slides***	***Formalin-fixed paraffinized microorganisms***
Gram-positive bacteria		
Lactobacillus sp.	–	ND
Streptococcus aureus	–	–
Gram-negative bacteria		
Burkholderia pseudomallei (2 strains)	+	+
Burkholderia thailandensis	+	+
Burkholderia cepacia	–	ND
Aeromonas hydraphila	–	–
Acinetobacter calcoaciniticus	–	–
Escherichia coli	–	–
Klebsiella pneumoniae	–	–
Neisseria gonorrhoeae	–	ND
Pseudomonas aeruginosa	–	ND
Proteus sp.	–	–
Salmonella enteriditis	–	–
Salmonella paratyphi	–	–
Shigella sonnei	–	–
Actinomyces spp.[a]	ND	–
Helicobacter pylori[a]	ND	–
Mycobacterium tuberculosis[a]	ND	–
Fungus		
Candida albicans	–	ND

Abbreviations: ND, not done; +, positive; –, negative.

[a] *Actinomycesspp*, *H. pylori*, and *M. tuberculosis* were human surgical biopsies in which these infections were confirmed.

APPENDIX 3

Hybridization buffer	20 X SSC	0.30ml
	50 X Denhardts solution	0.10ml
	Denatured Salmon sperm DNA	0.01ml
	DEPC treated dH_2O	0.09ml
	10% Dextran sulphate	0.50ml

The solution were added together and mixed well. DIG-labeled DNA probe was added to final concentration of ~1ng/ml. The mixture was prepared fresh before use.

Case No.	HPE No.	Hospital	Sex/ Age	Tissue	ZN	PAS/ GMS	Culture site	ISH results
1	S7378/11	HPP	M/36	Dura and brain tissue	-	-	tissue, swab	-
2	S5642/11	HPP	M/25	Liver	-	-	blood, tissue, pus, tracheal aspirate, fluid, swab	-
3	S5879/12	HPP	M/48	Lung	-	-	blood, tissue, tracheal aspirate	+
4	S1568/12	HPP	F/44	Synovium	ND	ND	tissue	-
5	S9237/13	HPP	M/73	Synovium	-	-	tissue, blood	-
6	S6626/12	HPP	F/30	Gluteal tissue	-	-	tissue	-
7	S4739/13	HPP	F/31	Spleen	-	-	pus, blood, tissue	-
8	S6719/12	HPP	M/6	Lymph nodes	-	-	pus	-
9	S1778/13	HPP	M/28	Pleura	ND	ND	fluid, swab	-
10	S0004/14	HPP	F/47	Spleen	ND	ND	blood	+
11	S7219/11	HPP	M/26	Pleura	-	-	pleural fluid	-
12	S10940/08	HPP	M/27	Spleen	ND	ND	blood	-
13	S6272/09	HPP	M/59	Testis	ND	ND	swab	-
14	S7429/13	HPP	M/56	FNAC of right parotid swelling (cell block)	ND	ND	blood, fluid	-
15	R0060/15	HPP	M/51	Lung	-	-	blood	-
16	N2180/15	HPP	F/50	Synovial fluid cytology (cell block)	ND	ND	blood	-
17	S8327/15	HPP	M/72	Scalp tissue and bone	-	-	pus	-
18	S2030/16	HPP	M/46	Cervical spine	-	-	bone	-
19	S2133/16	HPP	M/31	Thigh tissue	-	-	tissue	-
20	1407180	HRPBI	F/57	Labial tissue	ND	ND	blood	-
21	1308782, 01402935	HRPBI	M/50	C1-C6 epidural tissue	-	-	pus	-
22	1409022	HRPBI	M/67	Gastric tissue	ND	ND	blood	-
23	1007580	HRPBI	M/53	Bone	ND	ND	blood	-
24	1102281	HRPBI	M/48	Scalp tissue	ND	ND	blood	-
25	1501272	HRPBI	M/50	Knee tissue	ND	ND	blood	-
26	H05400/11	HSAJB	M/19	Bone marrow	-	-	blood	-
27	S2011/7686	UMMC	M/54	Spleen	-	-	Pus	+

Abbreviations: ND, not done; +, positive; -, negative

HPP, Hospital Pulau Pinang; HRPBI, Hospital Raja Permaisuri Bainun Ipoh; HSAJB, Hospital Sultanah Aminah Johor Bahru